

Air-sea exchange of acetone, acetaldehyde, DMS and isoprene at a UK coastal site.

Daniel P. Phillips¹², Frances E. Hopkins¹, Thomas G. Bell¹, Peter S. Liss², Philip D. Nightingale¹²³, Claire E. Reeves², Charel Wohl¹², Mingxi Yang¹

5 ¹Plymouth Marine Laboratory, Plymouth PL1 3DH, UK

²Centre for Ocean and Atmospheric Sciences, School of Environmental Sciences, University of East Anglia, Norwich NR4 7TJ, UK

³Sustainable Agriculture Systems, Rothamsted Research, Devon EX20 2SB, UK

Correspondence to: Daniel Phillips (dph@pml.ac.uk) and Mingxi Yang (miya@pml.ac.uk)

10 Abstract

Volatile organic compounds (VOCs) are ubiquitous in the atmosphere and are important for atmospheric chemistry. Large uncertainties remain in the role of the ocean in the atmospheric VOC budget because of poorly constrained marine sources and sinks. There are very few direct measurements of air-sea VOC fluxes near the coast, where natural marine emissions could influence coastal air quality (i.e. ozone, aerosols) and terrestrial gaseous emissions could be taken up by the coastal seas.

15 To address this, we present air-sea flux measurements of acetone, acetaldehyde and dimethylsulfide (DMS) at the coastal Penlee Point Atmospheric Observatory (PPAO) in the south-west UK during the spring (Apr-May 2018). Fluxes of these gases were measured simultaneously by eddy covariance (EC) using a proton transfer reaction quadrupole mass spectrometer. Comparisons are made between two wind sectors representative of different air-water exchange regimes: the open water sector facing the North Atlantic Ocean and the terrestrially influenced Plymouth Sound fed by two estuaries.

20 Mean EC (± 1 standard error) fluxes of acetone, acetaldehyde and DMS from the open water wind sector were -8.0 ± 0.8 , -1.6 ± 1.4 and $4.7 \pm 0.6 \mu\text{mol m}^{-2} \text{ d}^{-1}$ respectively (- sign indicates net air-to-sea deposition). These measurements are generally comparable (same order of magnitude) to previous measurements in the Eastern North Atlantic Ocean at the same latitude. In comparison, the Plymouth Sound wind sector showed respective fluxes of -12.9 ± 1.4 , -4.5 ± 1.7 and $1.8 \pm 0.8 \mu\text{mol m}^{-2} \text{ d}^{-1}$. The greater deposition fluxes of acetone and acetaldehyde within the Plymouth Sound were likely to a large 25 degree driven by higher atmospheric concentrations from the terrestrial wind sector. The reduced DMS emission from the Plymouth Sound was caused by a combination of lower wind speed and likely lower dissolved concentrations as a result of the estuarine influence (i.e. dilution).

30 In addition, we measured the near surface seawater concentrations of acetone, acetaldehyde, DMS and isoprene from a marine station 6 km offshore. Comparisons are made between EC fluxes from the open water and bulk air-sea VOC fluxes calculated using air/water concentrations with a two-layer (TL) model of gas transfer. The calculated TL fluxes agree with the EC measurements with respect to the directions and magnitudes of fluxes, implying that any recently proposed surface emissions of acetone and acetaldehyde would be within the propagated uncertainty of $2.6 \mu\text{mol m}^{-2} \text{ d}^{-1}$. The computed transfer 35 velocities of DMS, acetone, and acetaldehyde from the EC fluxes and air/water concentrations are largely consistent with previous transfer velocity estimates from the open ocean. This suggests that wind, rather than bottom-driven turbulence and current velocity, is the main driver for gas exchange within the open water sector at PPAO (depth of ~20 m).

1 Introduction

Volatile organic compounds (VOCs) are ubiquitous in the atmosphere and play an important role in atmospheric chemistry and carbon cycling in the biosphere (Heald et al., 2008). Many VOCs can influence the oxidative capacity of the atmosphere

40 by acting as a source or sink of atmospheric ozone (O_3) and hydroxyl radicals (Atkinson, 2000; Lewis et al., 2005), thereby influencing local air quality. The lower-volatility oxidation products, produced from reactions of some VOCs with atmospheric oxidants, can condense into particulates and form cloud condensation nuclei (CCN) (Charlson et al., 1987; Blando and Turpin, 2000; Henze and Seinfeld, 2006), affecting the Earth's radiative forcing and climate.

45 The terrestrial environment is the largest source of VOCs to the atmosphere with the emission dominated by isoprene from plant foliage (Guenther et al., 2006). Terrestrial biological processes also produce carbonyls including ketones and aldehydes in varying amounts (Kesselmeier and Staudt, 1999). Large uncertainties exist however with respect to the role that the ocean plays as a net source or sink of these gases (Broadgate et al., 1997; Arnold et al., 2009; Millet et al., 2010; Fischer et al., 2012; Wang et al., 2019). This is due to poorly quantified air-sea fluxes as well as uncertainties in the biogeochemical and physical processes that control them.

50 Acetone and acetaldehyde are carbonyl-based VOCs that have been shown to make up to ~57 % of the carbon mass of all non-methane organic carbon compounds in remote marine air over the North Atlantic Ocean (Lewis et al., 2005). These VOCs have been detected in the surface ocean at concentrations of up to tens of nM (Zhou and Mopper, 1997; Williams et al., 2004), with known oceanic sources including the photochemical degradation of dissolved organic matter (DOM) in bulk seawater (Kieber et al., 1990; Zhou and Mopper, 1997; Zhu and Kieber, 2018) and possibly autotrophic/heterotrophic biological processes (Halsey et al., 2017; Schlundt et al., 2017). The heterogeneous oxidation of DOM at the sea surface has recently 55 been identified as a source of carbonyl-containing VOCs (Zhou et al., 2014; Ciuraru et al., 2015), however the significance of this is currently unknown.

50 Dimethylsulfide (DMS) is a biogenic sulfur-containing VOC that constitutes the majority of the organic sulfur in the atmosphere (Andreae et al., 1985). It is produced in the surface ocean from the degradation of the algal osmolyte dimethylsulfoniopropionate (Kiene et al., 2000) and subsequently emitted into the atmosphere. DMS is often the dominant 60 source of sulfur in the marine atmosphere (Yang et al., 2011b), and the oxidation products of DMS can act as CCN (Charlson et al., 1987; Veres et al., 2020).

65 Isoprene is an unsaturated terpene-based VOC that is produced in the ocean by a broad range of phytoplankton as a secondary metabolic product (Moore et al., 1994; Shaw et al., 2003; Exton et al., 2013; Booge et al., 2016; Dani and Loreto, 2017). Oceanic sources of isoprene are important for the remote marine atmosphere (Lewis et al., 2001; Arnold et al., 2009; 70 Booge et al., 2016) where transport from terrestrial sources is negligible due to isoprene's very short atmospheric lifetime (~30 min; Carslaw et al., 2000).

70 The main oceanic sink of most VOCs is biological metabolism at varying rates (Dixon et al., 2014; Royer et al., 2016; Halsey et al., 2017). Surface seawater concentrations of acetone and acetaldehyde tend not to be very sensitive towards their air-sea fluxes (Beale et al., 2015). Emission to the atmosphere is generally considered to be a small loss for seawater DMS (Yang et al., 2013b) but a much larger loss relatively for seawater isoprene (Booge et al., 2018).

75 There have been very few direct measurements of air-sea VOC fluxes with the eddy covariance (EC) technique (e.g. Marandino et al., 2005; Yang et al., 2013c, 2014b; Kim et al., 2017). More often, the fluxes are estimated with the bulk method using air/sea concentrations in a two-layer (TL) model (e.g. Baker et al., 2000; Beale et al., 2013; Wohl et al., 2020). Most studies focus on open ocean air-sea exchange, while air-sea VOC flux measurements from the coast are essentially non-existent (EC or bulk). Compared to the open ocean, the coastal waters tend to be very dynamic biogeochemically (Borges et al., 2005; Bauer et al., 2013) and physically. For example, riverine runoffs carry nutrients and organic carbon into the coastal seas, which could stimulate intense biological cycling (Cloern et al., 2014). Furthermore, compared to the remote marine atmosphere, coastal air is affected by terrestrial emissions.

80 The air-sea gas transfer velocity can be derived by equating the EC flux with the bulk TL flux (e.g. Blomquist et al., 2010; Bell et al., 2013; Yang et al., 2013a, 2014a). Limited studies have been undertaken to identify whether open-ocean derived parameterisations of the transfer velocity are applicable to coastal systems (Borges et al., 2004; Yang et al., 2019a). Turbulent

processes (i.e. wave-breaking, tidal currents, bottom driven turbulence) are expected to behave differently in these environments (Upstill-Goddard, 2006), with potential impacts on gas exchange.

Here we present air-sea fluxes of acetone, acetaldehyde and DMS determined using the EC technique at a coastal observatory in the south-west UK. Using seawater concentrations measured from a marine station 6 km offshore, we further compute the TL fluxes of these VOCs as well as that of isoprene. We compare our coastal flux measurements with previous observations of open ocean fluxes as well as global model estimates. From the EC fluxes and air/sea concentrations, we derive the gas transfer velocities of DMS, acetone, and acetaldehyde and compare them against previous observations from the open ocean.

90 **2 Method**

2.1 Location

The Penlee Point Atmospheric Observatory (PPAO) is a long-term monitoring station and a part of the Western Channel Observatory (WCO; <https://www.westernchannelobservatory.org.uk/penlee/>) on the south-west (SW) coast of the UK (50.318° N, -4.189° E). The suitability of the observatory for direct air-sea exchange measurements (momentum, heat, 95 greenhouse gases, sea spray aerosols, O₃) has been discussed in detail before (Yang et al., 2016a, 2016c, 2019a, 2019b; Loades et al., 2020). The PPAO is located on an exposed headland that is exposed to two distinct wind sectors representative of different air-sea exchange regimes. The SW open water sector (depth of ~20 m within the flux footprint) faces the western English Channel and North Atlantic Ocean. The north-east (NE) Plymouth Sound sector (fetch-limited with a depth of ~10 m) is influenced by estuarine output from the rivers Tamar and Plym (Uncles et al., 2015) as well as natural terrestrial and 100 anthropogenic atmospheric emissions. The theoretical extent of the flux footprint at the PPAO has been discussed previously (Yang et al., 2019a; Loades et al., 2020).

2.2 Set-up and measurements

The EC system here principally consists of a high sensitivity proton transfer reaction – mass spectrometer (PTR-quadrupole-MS, Ionicon Analytik) and a sonic anemometer (Gill Windmaster Pro). The measurement setup closely followed previous 105 PPAO flux campaigns (Yang et al., 2016a, 2016d), with a few adaptations made to accommodate the PTR-MS requirements. A simple gas flow diagram is shown in Fig. 1.

The sonic anemometer was mounted on a mast ~19 m above mean sea level and run at 10 Hz. The air inlet consisted of a downwards-facing 90 ° union, mounted 30 cm below the anemometer, connected via a 10 m tube to a union tee upstream of the air pump (UT1). All PPAO air sampling instruments (including the PTR-MS) sub-sampled ambient air from this union tee. 110 A dry pump (Gast 1023 series) was used to draw ambient air into the observatory. The total flow rate was ~13.5 L min⁻¹, as calculated from the continuously monitored flow of the pump (Bronkhurst EL-FLOW series) and the sum of independent flows of connected instruments. All unions and tubing before UT1 were 9.5 mm internal diameter (ID).

Downstream of UT1 (i.e. closer to the instruments) was a 0.3 m, 3.2 mm ID tube and union tee (UT2), which split the sample air between the PTR-MS and other equipment (see Loades et al. (2020) for simultaneous PPAO O₃ fluxes). 115 Downstream of UT2 (i.e. closer to the PTR-MS) was a 0.3 m, 1.6 mm ID tube, which connected through a solenoid valve (Takasago Electric, Inc.) to the 1.2 m, 0.8 mm ID PTR-MS inlet tubing. All tubing, unions, fittings between the mast inlet and PTR-MS inlet were made from perfluoroalkoxy, while the solenoid valve was polytetrafluoroethylene and the PTR-MS inlet was polyetheretherketone (heated to 80 °C to limit surface adsorption).

A solenoid valve, controlled from the PTR-MS, was used to automate routine hourly blanking for the VOC measurements. 120 At the beginning of the campaign, sample gas (ambient air) was diverted through a platinum catalyst (heated to 450 °C) to produce VOC-free air (full oxidation to CO₂; Yang and Fleming, 2019). However, the use of the catalyst caused overheating

within the PPAO building and was replaced with an activated charcoal filter, which unfortunately proved to be inefficient at removing VOCs. The charcoal filter was replaced with compressed clean air (BOC synthetic air) towards the end of the campaign (27/04/18–03/05/18), which yielded the most consistent blanks. Post-campaign experiments show that the 125 acetaldehyde background when measuring dry, CO₂-free compressed air is lower than measuring moist atmospheric air scrubbed by the catalyst by about 0.33 ppbv (Wohl et al., 2020). This difference is due to the different levels of CO₂ (accounting for ~0.3 ppbv) and to a lesser extent water vapor (accounting for ~0.03 ppbv) between the compressed air and ambient air, qualitatively consistent with previous works (Warneke et al., 2003; Schwarz et al., 2009). Our calculation of atmospheric 130 acetaldehyde mixing ratio accounts for these sensitivities. Overall, the determination of the VOC backgrounds were more uncertain during this campaign than in previous measurements (Yang et al., 2013c), however, this is not expected to significantly influence the EC fluxes since the air concentrations were detrended during the flux calculation (Sect. 2.4).

The PTR-MS was set to multiple ion detection mode with four VOCs of interest: acetaldehyde, acetone, DMS and isoprene (initially at *m/z* 45, 59, 63 and 69 respectively). Previous experiments (Schwarz et al., 2009) and our laboratory tests (Wohl et al., 2019) show that substantial isoprene fragmentation occurs at the voltage used in these measurements (690 V, 166 Td). 135 Importantly, the *m/z* 41 fragment ion was shown to provide a larger and more stable signal than that of the isoprene parent ion (*m/z* 69). As a result, a week into the campaign the monitoring of isoprene was changed to *m/z* 41. The calibration (Sect. 2.5) and thus calculation of the isoprene mixing ratio accounted for the fragmentation and the change in ion monitored. The quadrupole mass dwell time was set to 50 ms for H₃O⁺ and 100 ms for each VOC. In total, the full ion cycle was just over 450 ms, which resulted in a sampling frequency of 2.2 Hz. Dwell time for each VOC was a compromise between measurement 140 frequency and instrument noise. The PTR-MS parameters are listed in Table A1. Data from the sonic anemometer, flow meter and PTR-MS were all recorded on the same computer to avoid desynchronisation.

2.4 Eddy covariance flux calculation

EC gas fluxes (*F*) are determined from the correlation between rapid changes (at least a few Hz) in vertical wind velocity (*w*) and the gas mixing ratio (*x*); $F = \rho_a \overline{w'x'}$, where ρ_a represents dry air density, the primes represent fluctuations from the 145 mean and the overbar represents temporal averaging. Air density was computed using the PPAO air temperature, pressure and humidity data (Gill Instruments Metpak Pro). Wind measurements were linearly interpolated from 10 Hz to match VOC measurement frequency.

A double wind rotation (Tanner and Thurtell, 1969; Hyson et al., 1977) was applied to each 10 min segment of wind data (u and v = horizontal, w = vertical), such that *u* became the wind speed (*U*) in the mean wind direction and *v* and *w* each 150 averaged zero. This was done to minimise the effect of flow distortion caused by the headland.

A lag time of approximately 3.5 s between wind and PTR-MS measurements was calculated from the dimensions of the tubing and flow rate. The lag time was further determined hourly using a lag correlation analysis between *w* and *x* over a window of +10 s. Acetone had the strongest flux signal of the four VOCs measured and was used to determine the lag time.

Lag-adjusted PTR-MS data were used to calculate fluxes in 10 min segments, the sampling interval chosen as the best 155 compromise between maintaining sufficient flux signal-to-noise ratio and satisfying the stationarity criteria in this dynamic region (Yang et al., 2016a, 2016c, 2019a, 2019b).

The sampling frequency of the PTR-MS is relatively low (2.2 Hz), and the instrument's response time determined from laboratory tests is just under 0.5 s. The computed fluxes were corrected for high frequency signal loss due to: 1) sampling at 2.2 Hz, and thus missing the flux above the Nyquist frequency of 1.1 Hz and 2) attenuation due to the tubing, using a combined 160 wind speed dependent attenuation factor (mean 1.09, max 1.18). This signal attenuation was estimated from the instrument's response time following the approach of Yang et al. (2013a).

The 10 min flux segments that met the quality control criteria (Table A2 for criteria details) were averaged into 1 h or 3 h fluxes, which reduces random noise by a factor of $\sim\sqrt{6}$ and $\sim\sqrt{18}$, respectively. Over the entire duration of the campaign, 61

% of the data were discarded mainly due to inappropriate wind directions (i.e. from land) or large variability in wind direction
165 (more common at low wind speeds). Diurnal variability was apparent in the open water wind sector data (SW winds) with respect to the number of acceptable flux segments. About twice as many flux segments passed quality control in the daylight hours compared to at night, which is likely due to a diurnal sea-breeze effect. When EC fluxes were averaged across 5 weeks of measurements, no difference was observed per hour of the day. No diurnal cycle could be seen in the Plymouth Sound wind sector data (NE winds), likely in part due to the limited data size.

170 Cospectra of acetone and DMS averaged over all quality-controlled periods are shown in Fig. 2 for both the open water and Plymouth Sound wind sectors. Here the areas between the cospectral curves and zero represent the magnitudes of the fluxes. Theoretical cospectral fits constrained by the actual wind speed and measurement height (Kaimal et al., 1972) suggest that the measured cospectral shapes were reasonable. The Kaimal fits also showed the high frequency flux loss ($>\sim 1$ Hz) was small, consistent with the estimated high frequency signal loss correction. Acetaldehyde and isoprene are not shown here because the
175 bidirectionality in acetaldehyde flux and the low isoprene flux magnitude (Sect. 3.1) cause very noisy cospectra.

2.5 Seawater measurements and two-layer flux calculation

Discrete seawater samples were collected from the L4 marine time-series station of the WCO, which is ~ 6 km S–SW of the PPAO headland. The near surface VOC concentrations are presumed to be similar between L4 and the PPAO open water flux footprint despite the outflow from the Tamar estuary that hugs the PPAO headland (Uncles et al., 2015); we revisit this
180 assumption in Sect. 3.3. Seawater acetaldehyde, acetone, DMS and isoprene concentrations were determined using a segmented flow coil equilibrator coupled to the PTR-MS before and after the PPAO campaign (following Wohl et al. (2019)). Additional seawater DMS concentration measurements were made weekly at L4 using gas chromatography (following Hopkins and Archer (2014)) for the Mar–May 2018 period.

Atmospheric VOC mixing ratios were blank-corrected using the synthetic gas cylinder measurements (27/04/18 onwards,
185 see Sect. 2.2), accounting for the humidity dependence in the background of DMS (mean correction 0.22 and 0.12 ppbv, for SW and NE air respectively, estimated from Wohl et al. (2019)) and the CO_2 plus humidity dependences in the background of acetaldehyde (constant correction 0.33 ppbv estimated from data from Wohl et al. (2020)). We have greater confidence in the measured atmospheric VOC mixing ratios after switching to synthetic air for the blank measurement. Thus, the EC fluxes and the two layer (TL) bulk fluxes were compared over this period (27/04/18–03/05/18) only. Gas phase calibrations of the PTR-
190 MS (using a certified gas standard, Apel-Riemer Environmental Inc) before and after the deployment were averaged and applied to both the atmospheric and seawater VOC data.

Surface saturation values of DMS and acetaldehyde were calculated using the recommended solubility from the literature (Burkholder et al., 2015; Sander, 2015) as a function of temperature and adjusted for salinity (Johnson, 2010). Recent calibrations at environmentally relevant concentrations in seawater suggest that acetone is less soluble than previously thought
195 (Wohl et al., 2020); thus the acetone air-over-water solubility recommended by Burkholder et al. (2015) was divided by 1.4 as recommended by Wohl et al. (2020).

The calculation of the bulk TL fluxes requires the use of wind speed dependent gas transfer velocity parametrisations. The measured wind speed at the PPAO was corrected for flow acceleration due to the headland using results from a comparison with a wind sensor on the L4 buoy (Yang et al., 2019a). This scaled the wind speeds from 19 m (height of the PPAO mast) to
200 4.9 m (height of L4 wind sensor), and also removed the effect of wind acceleration from the sloped PPAO headland. The corrected winds were then scaled to 10 m; $U_{10} = U_{4.9}(\ln(10/z_0)/\ln(4.9/z_0))$, where z_0 represents the aerodynamic roughness length calculated from U using the COAREG 3.5 model (Edson et al., 2013). Overall, the mean correction factor was 0.93 (min 0.79 and max 1.39) for the two wind sectors. The relationship between the corrected U_{10} and EC friction velocity ($u_* = ((\bar{u}'w')^2 + (\bar{v}'w')^2)^{0.25}$) shows reasonable agreement with the COAREG 3.5 model as well as with Mackay and Yeun
205 (1983) (Fig. S1), which validate these wind corrections.

Bulk fluxes (F) were calculated following Liss and Slater (1974) and Johnson (2010);

$$F = -K_a(C_a - HC_w) \quad (1)$$

$$K_a = \left(\frac{1}{k_a} + \frac{H}{k_w} \right)^{-1} \quad (2)$$

where K_a represents total airside transfer velocity, C_a and C_w represent air and waterside concentrations respectively, H represents air-over-water dimensionless Henry solubility and k_a and k_w represent the individual air and waterside transfer velocities, respectively. Note that total waterside transfer velocity (K_w), more commonly used for waterside controlled gases such as DMS and isoprene, is equal to HK_a . k_a was calculated from the COAREG 3.5 model (Edson et al., 2013), which can be approximated as $k_a \approx -0.32884U_{10}^{-3} + 27.428U_{10}^{-2} + 34.936U_{10}^{-1} + 553.71$. The VOCs targeted here span only a small range in diffusivity in air, and are thus assumed to have the same k_a for simplicity (Yang et al., 2014a, 2016b). k_w for acetone, 210 acetaldehyde and DMS was calculated using the fit from Yang et al. (2011a); this was an average of DMS observations from five cruises: $k_w \approx (-0.00797U_{10}^{-3} + 0.208U_{10}^{-2} + 0.484U_{10}^{-1})(S_{Cw}/660)^{-0.5}$, where S_{Cw} represents waterside Schmidt 215 number. k_w for isoprene was calculated using the fit from Nightingale et al. (2000); $k_w \approx (0.222U_{10}^{-2} + 0.333U_{10}^{-1})(S_{Cw}/600)^{-0.5}$. At a U_{10} of 10 m s⁻¹, the Nightingale et al. (2000) parametrization would overestimate DMS k_w by ~37 % because bubble-mediated gas exchange is less important for the moderately soluble DMS (see Bell et al., 2017; Blomquist et al., 2017). 220 The waterside Schmidt number for all gases were computed following Johnson (2010) at the ambient temperature and salinity.

Appendix B provides further information on the chosen gas solubilities, waterside data and calculations.

3 Results and Discussion

3.1 EC fluxes for the open water and Plymouth Sound wind sectors

Flux measurements were made between 05/04/18 and 03/05/18. During this period, winds arrived from the open water wind 225 sector (180–240° N) 30 % of the time and from the Plymouth Sound sector (30–70° N) 8 % of the time. The wind directions defining these two marine flux sectors were re-established (see Appendix C) compared to previous PPAO studies after raising the mast height by ~1 m at the beginning of this campaign.

A time series of VOC fluxes (3 h average) is shown in Fig. 3. While acetone and DMS had clear unidirectional fluxes (deposition and emission respectively), acetaldehyde showed bidirectional fluxes throughout the campaign. EC fluxes of 230 acetone, acetaldehyde, DMS and isoprene from the two marine wind sectors averaged over the entire campaign are summarised in Table 1, with positive fluxes representing net sea-to-air emission.

For the open water sector, acetone and DMS fluxes had relative standard errors <12 % (from 1 h bins), which are confidently 235 represented by the measurements in the mean thanks to the robust signal-to-noise ratio. Acetaldehyde had a much greater relative standard error (74 %) because the fluxes often changed in direction and were smaller in magnitude (closer to the limits of detection, LOD); acetaldehyde standard error is lowered to 51 % when the 573 10 min flux segments are instead averaged over the campaign. The isoprene flux was not resolvable with the EC method using our PTR-MS due to the low signal-to-noise ratio. The only direct measurement of isoprene flux from the sea (Kim et al. (2017) in the North Atlantic Ocean) used a chemical ionisation mass spectrometer that is significantly more sensitive than the PTR-MS here.

Overall, 68, 33, 62 and 35 % of 3 h averages of acetone, acetaldehyde, DMS and isoprene, respectively, were above the 240 LOD (DMS and isoprene had the additional condition of a positive flux above LOD) for the open water sector. The estimation of LOD is shown in Appendix A.

The greater air-to-sea deposition fluxes of acetone and acetaldehyde in the Plymouth Sound sector, compared to the open water sector, were likely driven by the higher gas mixing ratios in terrestrially-influenced air. Distributions of atmospheric acetone mixing ratio from the two wind sectors are shown in Fig. 4. Seawater concentrations of acetone and acetaldehyde 245 within the Plymouth Sound flux footprint were not measured, and thus we are unable to comment on the quantitative effect of

riverine outflow on the dissolved VOC concentrations. The weaker sea-to-air flux of DMS in the Plymouth Sound sector compared to the open water sector was likely due to a combination of low DMS water concentrations associated with freshwater outflow (Uncles et al., 2015) and lower wind speed (Fig. 4) that results in reduced gas transfer velocity (k_w ; Nightingale et al., 2000; Yang et al., 2011a).

250 3.2 Seawater concentration and atmospheric mixing ratios of VOCs

The seawater concentrations of acetone, acetaldehyde and DMS measured around the campaign (Table A4) are broadly similar ($\leq 48\%$ difference) to previous measurements in the Western English Channel (Archer et al., 2009; Beale et al., 2015), a highly variable and seasonal environment. No seawater measurements of isoprene have been published in this region, so comparisons are made to previous observations from the eastern North Atlantic (~ 0.02 nM; Broadgate et al., 2004; Hackenberg et al., 2017), which are $\sim 79\%$ lower than measurements here. The eastern North Atlantic measurements were conducted in Sep–Oct, thus likely represent a period of lower isoprene productivity. An annual study in the North Sea found the highest isoprene seawater concentrations in May (~ 0.06 nM; Broadgate et al., 1997), which were closer to our L4 measurements but still lower ($\sim 41\%$).

The mean atmospheric mixing ratios of acetone and acetaldehyde from the open water sector (0.82 ± 0.16 and 0.51 ± 0.07 ppbv respectively, Table 2) are greater than previous measurements around the sample site, possibly in part due to our measurements occurring mainly over one day (1st May 2018; see Fig. 6 later for timeseries) thus a multiday average was not possible. Remote marine Atlantic Ocean measurements from the ATom-4 campaign (Apr–May 2018), within 0.5 km of the sea surface and at latitudes of 40–60° N, observed 0.31 ± 0.01 ppbv acetone (\pm SD) and 0.15 ± 0.04 ppbv acetaldehyde (Wofsy et al., 2018). Better agreement was seen with shipboard measurements between 40 and 50° N in the eastern North Atlantic Ocean (Yang et al., 2014b) and coastal measurements at the Mace Head Observatory (Lewis et al., 2005) with mean acetone mixing ratios of ~ 0.65 and 0.50 ppbv, respectively, and acetaldehyde mixing ratios of ~ 0.16 and 0.44 ppbv, respectively. Finally, rooftop measurements at PML (~ 350 m north of the Plymouth Sound, ~ 6 km NE of the PPAO, and affected by local ship/port activities) showed night time atmospheric mixing ratios of ~ 0.4 and ~ 0.1 ppbv, respectively for acetone and acetaldehyde (Yang et al., 2013c). A summary of these concentrations, in coordinate form, can be found in Fig. S3. The atmospheric carbonyl measurements at the PPAO from this day might not represent purely oceanic conditions even though wind was from the open water sector. Hysplit (Stein et al., 2015; Rolph et al., 2017) backward trajectories suggest that the air mass sampled on 1st May 2018 made contact with land (mainland UK) ~ 24 – 48 h prior to arriving at the PPAO (Fig S4). Lewis et al. (2005) show that similar air-mass trajectories over the UK and continental Europe contained high acetone levels (max of ~ 1.67 ppbv).

275 Our mean DMS mixing ratio (0.20 ± 0.09 , Table 2) is in agreement with shipboard measurements in the eastern North Atlantic Ocean in Jun/Jul (0.16 ± 0.14 and 0.12 ± 0.08 ppbv (Huebert et al., 2010), with and without a phytoplankton bloom, respectively) and the western North Atlantic Ocean in March ($\sim 0.13 \pm 0.04$; Quinn et al., 2019). Our mean isoprene mixing ratio (0.18 ± 0.05) is higher than observations in autumn from the western North (0.035 ± 0.025 ppbv; Kim et al., 2017) and eastern North (0.0044 ± 0.0083 ppbv; Hackenberg et al., 2017) Atlantic Ocean. The PPAO isoprene mixing ratio is more similar to measurements at the Mace Head Observatory (Carslaw et al., 2000), which further implies some influence from terrestrial land sources at the PPAO site. We note that the TL air–sea isoprene flux is almost purely governed by its seawater concentration where it is grossly supersaturated; the flux is insensitive to the elevated atmospheric mixing ratio.

280 3.3 Comparison between EC and bulk TL fluxes and derivation of the gas transfer velocities

Here we compare EC fluxes of acetone, acetaldehyde and DMS from the open water sector with fluxes computed with the TL model (using concurrent atmospheric mixing ratios from the PPAO and linearly interpolated seawater concentrations from L4). This is to assess two assumptions in the TL flux calculation: 1) that gas transfer velocity parameterisations from deeper

water (i.e. the open ocean or shelf seas) are applicable to this shallower coastal environment, and 2) seawater VOC concentrations in the PPAO flux footprint and at the L4 station are similar.

Acetone and acetaldehyde were both undersaturated in seawater in the open water sector (Table 2), while DMS and isoprene were both supersaturated. The mean TL fluxes of acetone, acetaldehyde, DMS and isoprene (n=20) are provided in Table 2 with corresponding EC measurements from the open water wind sector for the last week of the campaign (27/04/18–03/05/18). For this short period with satisfactory VOC blanking, the open water EC fluxes were fairly large in part because of a 17 % higher mean wind speed compared to the rest of the campaign.

Figure 5 compares the VOC EC and TL fluxes for the open water sector (not inc. isoprene), and Fig. 6 shows the same data as a time series. Acetone, acetaldehyde and DMS fluxes exhibit reasonable agreement between the EC and TL methods, with both covarying with wind speed. The data points furthest from the 1:1 line in Fig. 5 are hourly averages with ≤ 10 min flux segments, suggesting that the discrepancy is mainly due to random noise in the flux measurement. We do not attempt to calculate TL fluxes for the Plymouth Sound sector because we do not have concurrent seawater measurements and have limited EC measurements for comparison.

To assess the wind speed dependence in gas transfer velocities at the PPAO, K_a is calculated by equating the EC flux with TL flux; $\rho_a \overline{w'x'} = -K_a(C_a - HC_w)$. Figure 7 shows the calculated K_a and K_w ($K_w = HK_a$) values for acetone, acetaldehyde and DMS using 1 h flux data, compared to calculated K from parameterisations of k_a and k_w . In the mean, the expected solubility-dependence in these VOCs is observed – the measurements show mean K_a of 2121, 1894 and 183 cm h⁻¹ for acetone, acetaldehyde and DMS (in order of decreasing solubility), respectively. These translate to K_w values of 2.0, 2.6 and 9.9 cm h⁻¹.

For DMS, to facilitate comparison with previous measurements, the derived K_w is adjusted to a standard Schmidt number of 660 ($K_{660} = K_w(660/S_{CW})^{-0.5}$). The mean K_{660} for DMS (16.7 \pm 2.7 cm h⁻¹) is in good agreement when compared to published measurements (\sim 17 cm h⁻¹; Blomquist et al., 2006; Yang et al., 2011a; Bell et al., 2013) at similar wind speeds in the North Atlantic Ocean. Data from this short campaign suggest that the mean wind speed dependence in DMS transfer velocity at the PPAO (open water sector, depth of \sim 20 m) is largely comparable to deeper water, in agreement with previous CO₂ gas exchange measurements at this site (Yang et al., 2019a). Our measured acetone and acetaldehyde K_a are also of the expected magnitudes. Processes important for shallow estuaries, such as bottom-driven turbulence and tidal current, do not appear to be the main controlling factors in gas exchange in this environment.

There is a large amount of scatter in Fig. 7, especially for acetone and acetaldehyde. This is likely in part due to the poor temporal resolution (weekly) in seawater concentration measurements that do not capture any rapid changes in this dynamic region (e.g. changes in riverine outflow, biological bloom). Our DMS transfer velocity measurements imply that the outflow of the estuary Tamar does not substantially dilute the seawater DMS concentration within the open water flux footprint compared to L4, while spatial gradients in the carbonyl concentrations could be more significant relative to their air/sea concentration differences. Higher resolution measurements within the flux footprints in the future are needed to better constrain the influence of riverine outflow.

As mentioned in Sect. 2.5, this paper uses a revised acetone solubility from Wohl et al. (2020). Focusing on the last week of the campaign (Table 2), we compute a mean TL acetone flux of -19.0 ± 2.2 and -21.5 ± 2.5 $\mu\text{mol m}^{-2} \text{d}^{-1}$ (\pm SD, propagated error in concentration only) with and without the solubility revision. The flux with revised solubility is in better agreement with the EC measurement (-14.9 ± 2.1 $\mu\text{mol m}^{-2} \text{d}^{-1}$).

3.4 Comparison to other flux estimates

The acetone fluxes presented here are in good agreement with previous EC measurements (-7.0 ± 2.2 $\mu\text{mol m}^{-2} \text{d}^{-1}$) from 50° N on an Atlantic Meridional Transect (AMT) research cruise in Autumn 2012 (Yang et al., 2014b). However, the acetaldehyde flux here shows an opposite mean direction to their 50° N average (1.8 ± 1.3 $\mu\text{mol m}^{-2} \text{d}^{-1}$). Acetone and acetaldehyde bulk fluxes from 50° N during an AMT cruise in 2009, estimated using CAM–Chem modelled atmospheric concentrations,

were -5.7 ± 1.1 and $-2.4 \pm 0.7 \text{ } \mu\text{mol m}^{-2} \text{ d}^{-1}$ respectively (Beale et al., 2013). The PPAO fluxes are in reasonable agreement with these earlier indirect estimates. Further acetone and acetaldehyde bulk fluxes estimated from a time series of L4 water measurements and static atmospheric mixing ratios (0.66 and 0.40 ppbv respectively) were -7.4 ± 1.4 and $1.4 \pm 1.0 \text{ } \mu\text{mol m}^{-2} \text{ d}^{-1}$, respectively, for spring 2011 and -6.4 ± 0.1 and $-1.5 \pm 0.1 \text{ } \mu\text{mol m}^{-2} \text{ d}^{-1}$, respectively, as annual averages. The spring acetone fluxes of Beale et al. (2015) are in good agreement with the PPAO direct measurements, however their acetaldehyde flux was in the opposite direction. Importantly, Beale et al. (2015) identified that the L4 water saturation of acetaldehyde was highly sensitive to the atmospheric mixing ratio (changing it between 0.1–0.4 ppbv was enough to switch the direction of flux). Thus variability and uncertainty in the atmospheric acetaldehyde mixing ratio are probably among the main causes for the discrepancies in these air–sea flux estimates (Yang et al. (2014b), Beale et al. (2013, 2015), and PPAO measurements presented here).

The PPAO DMS flux is in agreement with previous EC DMS flux observations from the Eastern North Atlantic Ocean during summer 2007 (2.6 ± 0.2 and $4.4 \pm 0.4 \text{ } \mu\text{mol m}^{-2} \text{ d}^{-1}$ with and without a short, intense phytoplankton bloom; Huebert et al., 2010). Our campaign ended before the spring phytoplankton bloom started at L4 (Archer et al., 2009), which typically starts in May/June. Yang et al. (2016c) estimated bulk DMS fluxes of 3 and $10 \text{ } \mu\text{mol m}^{-2} \text{ d}^{-1}$ in the winter and summer, respectively, using the L4 annual seawater DMS concentration time series (Archer et al., 2009). The DMS flux measurement at the PPAO is also in reasonable agreement with previous observations in the North Atlantic Ocean without the phytoplankton bloom ($5.58 \pm 0.15 \text{ } \mu\text{mol m}^{-2} \text{ d}^{-1}$; Bell et al., 2013).

Although isoprene EC fluxes were unresolvable, the estimated open water TL flux was similar to NECS April estimates of $\sim 0.8 \text{ } \mu\text{mol m}^{-2} \text{ d}^{-1}$ (Palmer and Shaw, 2005) and $\sim 1.0 \text{ } \mu\text{mol m}^{-2} \text{ d}^{-1}$ (Booge et al., 2016, supp.) using MODIS satellite observations of chlorophyll-a for production models. A mean direct flux ($0.7 \text{ } \mu\text{mol m}^{-2} \text{ d}^{-1}$) was observed in the eastern North Atlantic Ocean (Kim et al., 2017); they estimated seawater concentrations ($\sim 0.02 \text{ nM}$) that were $\sim 78 \text{ \%}$ lower than measured here but also experienced much higher wind speed. Importantly, discrepancies between top-down and bottom-up isoprene budget analyses show the ocean fluxes necessary to explain remote marine boundary layer (MBL) concentrations of isoprene are on the order of a magnitude higher than predicted from seawater concentrations alone (Arnold et al., 2009; Booge et al., 2016). Future simultaneous comparisons between EC and TL isoprene fluxes might observe this difference.

We also compare our direct VOC fluxes to global model predictions at this location. Typical global models and climatologies operate with a 1° latitudinal and longitudinal resolution (e.g. Wang et al., 2019, 2020a, 2020b). At the PPAO this equates to a grid size of $\sim 110 \text{ km N–S}$ and $\sim 85 \text{ km E–W}$, which is much coarser compared to the flux footprint areas (on the order of a few km^2). Nevertheless, this comparison allows us to qualitatively assess the spatial representativeness of the PPAO fluxes and identify potential shortcomings in the models.

The GEOS–Chem and CAM–Chem models predict a mean annual acetone flux in the Eastern North Atlantic Ocean coastal shelves (NECS; biogeochemical province that includes the PPAO coastal site) of $\sim 2.5 \text{ } \mu\text{mol m}^{-2} \text{ d}^{-1}$ (Fischer et al., 2012) and Mar–May flux of $\sim 2.9 \text{ } \mu\text{mol m}^{-2} \text{ d}^{-1}$ (Wang et al., 2020a), respectively. These two predictions are much lower than measured in the PPAO open water sector ($-8.01 \pm 0.77 \text{ } \mu\text{mol m}^{-2} \text{ d}^{-1}$, Table 1) because the models predict a smaller air–sea concentration difference. Fisher et al. (2012) and Wang et al. (2020a) used water concentrations of 15 (static) and $\sim 8 \text{ nM}$ respectively (182 % and $\sim 50 \text{ \%}$ higher than L4 concentrations) and a modelled atmospheric mixing ratio of $\sim 0.45 \text{ ppbv}$ ($\sim 45 \text{ \%}$ lower than the PPAO concentration). Seawater acetone has a highly variable lifetime (Beale et al., 2013; de Bruyn et al., 2013; Dixon et al., 2013) so the higher estimated seawater concentration in the Wang et al. (2020a) model may be because of a slower removal rate. We measured an atmospheric acetone mixing ratio that is higher than in the model likely because our measurement, even from the open water sector, has some terrestrial influence (e.g. via the diurnal sea-breeze effect or advection of air masses previously in contact with land).

The small negative acetaldehyde fluxes measured at the PPAO imply a weak ocean sink (mean of $-1.55 \pm 1.14 \text{ } \mu\text{mol m}^{-2} \text{ d}^{-1}$, Table 1), which does not agree with global model results. The NECS acetaldehyde flux is $\sim 0.22 \text{ } \mu\text{mol m}^{-2} \text{ d}^{-1}$ in GEOS–Chem

(Millet et al., 2010) and $\sim 1.4 \text{ } \mu\text{mol m}^{-2} \text{ d}^{-1}$ in CAM–Chem (Wang et al., 2019) in the Mar–May period. The seawater concentrations used by Wang et al. (2019) ($\sim 11 \text{ nM}$) are higher than L4 measurements for the same period (54 % higher than L4 conc.). In the model, the short marine lifetime of acetaldehyde (de Bruyn et al., 2013, 2017; Dixon et al., 2013) is coupled with an estimate of its production rate to predict the seawater concentration. Wang et al. (2019) use of a constant lifetime of 0.3 d for the global ocean, whereas previous measurements at L4 suggest a much shorter acetaldehyde lifetime (0.01–0.13 d; Beale et al., 2015). de Bruyn et al. (2017) showed shorter seawater acetaldehyde lifetimes at another coastal location directly after rainfall or during the wet season. It is possible that the shorter lifetime at L4/PPAO, and hence lower seawater acetaldehyde concentration, may be related to riverine input. The atmospheric acetaldehyde mixing ratios from the models are also lower than the coastal observations presented here, similar to acetone as discussed above.

From the perspective of climatology and global modelling, the NECS was predicted to have an April DMS flux of $\sim 14 \text{ } \mu\text{mol m}^{-2} \text{ d}^{-1}$ (Lana et al., 2011) and $\sim 6 \text{ } \mu\text{mol m}^{-2} \text{ d}^{-1}$ (Wang et al., 2020b). The estimate of Lana et al. (2011) is 3 times higher than the PPAO measurements, however that of Wang et al. (2020b) is in good agreement. Waterside concentrations of ~ 7 and $\sim 3 \text{ nM}$ were predicted (52 % higher and 43 % lower than the L4 concentration) by Lana et al. (2011) and Wang et al. (2020b) respectively. The high concentrations in the Lana et al. (2011) climatology likely correspond to phytoplankton blooms in the Apr–May period, which did not occur at the time of our measurements nor appear as intensely in the estimations of Wang et al. (2020b). This could be partly related to the interannual variability in plankton dynamics and hence seawater DMS cycling.

All the models and climatologies discussed here (except for Wang et al. (2020b)) used the Nightingale et al. (2000) k_w parameterisation, which leads to ~ 26 , ~ 14 and $\sim 26 \text{ %}$ higher k_w values for acetone, acetaldehyde and DMS, respectively, than that of Yang et al. (2011a) over this campaign because of the solubility dependence in bubble-mediated gas exchange (Yang et al., 2011a; Bell et al., 2017). Substituting the Nightingale et al. (2000) k_w parameterisation with the Yang et al. (2011a) k_w would generally reduce the flux magnitude in these models; estimated as ~ 5 , ~ 6 and $\sim 19 \text{ %}$ for acetone, acetaldehyde and DMS, respectively (k_a unchanged and from COAREG 3.5).

3.5 Significance of fluxes

Our measured open water acetone and acetaldehyde air–sea fluxes exhibit stronger deposition flux than estimated by global modelling. Here we evaluate the lifetimes of these gases within the atmospheric MBL. The MBL lifetimes (τ_x) are calculated similarly to a 0D model; $\tau_x = C_x / (C_x L_x + D_x / h)$, where C_x represents concentration (here, the mean of the PPAO observations, Table 2), L_x represents chemical loss, D_x represents the net deposition flux (here, the mean of the PPAO EC observations, Table 1) and h represents MBL height. We assume h to be 500 m and VOCs to be homogeneously mixed within the MBL upwind of the PPAO, and L_x is $2.7 \times 10^{-7} \text{ s}^{-1}$ for acetone and $2.1 \times 10^{-5} \text{ s}^{-1}$ for acetaldehyde. L_x is calculated from literature OH reaction rates (1.7×10^{-13} and $1.5 \times 10^{-11} \text{ cm}^3 \text{ molec.}^{-1} \text{ s}^{-1}$, respectively; Atkinson and Arey, 2003), April surface 50° N zonal average OH concentration ($\sim 10^6 \text{ molec. cm}^{-3}$; Horowitz et al., 2003) and summer surface photolysis rates for acetone ($\sim 10^{-7} \text{ s}^{-1}$; Blitz et al., 2004) and acetaldehyde ($\sim 5.5 \times 10^{-6} \text{ s}^{-1}$; Warneck and Moortgat, 2012).

From this simple model and the values described above, the MBL lifetimes of acetone and acetaldehyde are calculated to be 2.0 and 0.5 d respectively. The deposition to the ocean above accounts for 95 and 8 % of all losses for MBL acetone and acetaldehyde respectively, which highlights the importance of acetone air–sea exchange. The calculated PPAO open water acetone lifetime is much shorter than the 11–18 d estimates for the mean troposphere (Marandino et al., 2005; Fischer et al., 2012; Khan et al., 2015; Wang et al., 2020a), where surface deposition is less substantial (16–56 %; Jacob et al., 2002; Fischer et al., 2012). The acetaldehyde lifetime is in good agreement with literature values (0.1–0.8 d; Millet et al., 2010; Wang et al., 2019) because photochemistry is the main loss mechanism for MBL acetaldehyde rather than deposition, and the Apr surface 50° N zonal average OH concentration is similar to the tropospheric mean ($1.1 \times 10^6 \text{ molec. cm}^{-3}$; Li et al., 2018).

The noticeable increase in acetone and acetaldehyde deposition fluxes within the Plymouth Sound compared to the open water sector suggests that deposition can represent a large loss term for atmospheric VOCs in the coastal atmosphere.

Importantly, enhanced coastal deposition fluxes of acetone and acetaldehyde are not well captured in global models. The 415 boundary layer lifetimes during periods of offshore winds are calculated using the same approach as before, resulting in 1.7 d for acetone and 0.5 d for acetaldehyde. Here deposition to the ocean accounts for 96 and 17 % of losses, respectively. The estimated lifetimes in the Plymouth Sound sector are similar to the open ocean even though the deposition fluxes were stronger because the increased deposition fluxes correspond to a greater atmospheric burden. As airmasses from the Plymouth Sound 420 (or further inland to the NE) are advected offshore over the coastal seas, the mixing ratios of carbonyls tend to decrease due to combination of deposition to the sea, chemical losses, and mixing with marine air. If additional x-y dimensional constraints are added to the Plymouth Sound 0D box (e.g. 4 km N–S, 1 km E–W), dilution becomes an important loss term.

4 Conclusions

This paper presents measurements of air–sea fluxes of acetone, acetaldehyde and DMS at the coastal PPAO in the SW UK. A PTR-quadrupole-MS (2.2 Hz) was used to simultaneously resolve the fluxes of these gases with the eddy covariance method. 425 Comparisons between the open water sector and a terrestrially influenced sector show stronger deposition fluxes of acetone and acetaldehyde from the latter because of higher atmospheric carbonyl concentrations from that wind direction. Emission fluxes of DMS from the terrestrially influenced sector are weaker than from the open water sector, likely because of lower wind speeds and lower seawater concentrations due to estuarine influence/dilution.

Bulk fluxes computed from seawater and atmospheric concentrations using the TL approach agree reasonably well with our 430 EC measurements of open water acetone, acetaldehyde and DMS fluxes. The derived air–sea transfer velocities of acetone, acetaldehyde and DMS are largely consistent with previous estimates over the open ocean in the mean. Along with previous measurements of air–sea CO₂ exchange, these data suggest that wind, rather than processes such as bottom driven turbulence, is the dominant control for gas exchange at this site for the open water sector (depth of ~20 m).

While the DMS flux at PPAO was in reasonable agreement with recent climatological estimates, our measured open water 435 acetone fluxes show stronger deposition compared to climatological and model estimates for the NE Atlantic Ocean coastal shelf. This is likely because the models/climatologies do not fully capture the spatial and temporal variability in the distribution of atmospheric and seawater acetone concentrations. The PPAO acetaldehyde flux (net sink in the mean) is in the opposite direction to global models that suggest that the northern hemisphere oceans to be a net acetaldehyde source. This is mostly 440 because models predict higher seawater acetaldehyde concentrations and lower atmospheric acetaldehyde mixing ratios at this coastal location.

Future experiments at PPAO should strive to increase the temporal and spatial resolutions of the C_w observations in order 445 to better match up with the EC fluxes. The accuracies in the air/water concentration measurements can be further improved by using blanks that have the same CO₂ and humidity levels as the samples, especially for acetaldehyde. The use of a higher resolution PTR-time-of-flight-MS at ≥ 10 Hz would improve the precision of the flux measurement and reduce the magnitude of the high frequency flux loss. Simultaneous methanol fluxes would enable the derivation of the airside gas transfer velocity 450 (k_a) and benefit the lag correlation calculation (methanol flux is typically large; see Yang et al. (2014a)). Important future work would involve measuring EC fluxes, C_w and C_a at high resolution from the anthropogenically/terrestrially dominated coast through to the continental shelf edge and open ocean on a ship in order to develop our understanding of the impact of coastal seas on local atmospheric chemistry and quality. Such transect measurements would help to further constrain global

Appendix A: Additional eddy covariance method details

Table A1 shows the PTR-MS measurement parameters used, which largely follows from Yang et al. (2013c). Importantly, a high drift voltage was used to limit the formation of hydrated clusters ($H_3O^+ + nH_2O \rightarrow H_3O^+(H_2O)_n$) caused by the high humidity of marine air. These hydrated clusters have different reaction kinetics with VOCs and can affect the instrumental sensitivity. Increasing the drift voltage leads to a lower cluster formation, but also causes a greater degree of isoprene fragmentation (Schwarz et al., 2009; Wohl et al., 2019). Isoprene fragmentation was corrected using gas phase calibration.

Table A2 shows the quality control criteria used to filter 10 min flux data segments, developed from EC measurements of CO₂ and CH₄ fluxes at the PPAO (Yang et al., 2016a). Standard deviation in wind direction was used to ensure fairly constant wind direction and minimise influence from areas outside the specified NE and SW wind sectors. The remaining controls check for the stationary criteria required for EC measurements, remove periods with obvious flow distortion, or remove periods with substantial rain influence on the sonic anemometer.

Random uncertainty in the EC flux depends on variability (instrument noise + ambient variability) in the VOC measurement and the wind measurement. Precision (or random error) in the EC technique can be approximated as the standard deviation of ‘null’ fluxes (i.e. covariance data with a lag time between vertical wind and concentration measurements that is much greater than the integral time scale (Spirig et al., 2005)). Fluxes are resolvable when they are higher than 3x the measurement noise. An artificial lag time of 300 s was chosen for this calculation here. The 3x standard deviation was calculated from hourly averages over a 5 h window of stable open water wind speed and direction as 10.1, 6.8, 4.7 and 4.7 $\mu\text{mol m}^{-2} \text{ d}^{-1}$, for acetaldehyde, acetone, DMS and isoprene respectively. Our LOD estimates are 140–250% of the LODs from a previous deployment of this PTR-MS at sea (Yang et al., 2014b), mainly due to the greater ambient variability in VOC mixing ratio at this coastal environment. Averaging hourly data to 3 h reduces random error by a factor of $\sqrt{3}$, thus the 3 h LOD are 5.8, 4.0, 2.7 and 2.7 $\mu\text{mol m}^{-2} \text{ d}^{-1}$, for acetaldehyde, acetone, DMS and isoprene respectively.

Appendix B: Two-layer flux calculation additional information

Table A3 shows the solubility and solubility temperature dependence (Burkholder et al., 2015) and molar volume data (Johnson, 2010) used in the calculations of salinity dependent solubility and Schmidt number. In the diffusion coefficient calculation, the original association factor of solvent (2.6) was used as recommended by Saltzman et al. (Saltzman et al., 1993) for DMS.

During the period with satisfactory hourly blanking (27/04/18–03/05/18), the mean ($\pm\text{SD}$) L4 water temperature and salinity were $10.6 \pm 0.8^\circ\text{C}$ and 34.9 ± 0.1 PSU. These were taken from the surface measurement of a weekly CTD profile collected on the RV *Plymouth Quest*. Mean atmospheric pressure was 1006 ± 4 mB, wind speed at 10 m height was $9.93 \pm 3.76 \text{ m s}^{-1}$, and friction velocity (also from EC) was $0.364 \pm 0.166 \text{ m s}^{-1}$. Table A4 shows the available VOC concentration data just before, during and after the campaign. Simultaneous measurements and calculated fluxes were made using concentration data from as close as possible to the period with satisfactory blanking (*).

Appendix C: Wind sector determination

Figure S2 shows the double wind rotation tilt angle correction and drag coefficient ($C_D = (u_*/U)^2$) for 10 min segments of wind data averaged into wind direction bins. The 10 min data were filtered ($U > 3 \text{ m s}^{-1}$) to reduce the influence of the flux footprint overlapping with the narrow strip of land upwind under low wind speed conditions (Yang et al., 2019a). The majority of winds had a positive tilt angle due the rotation of ocean (horizontal) winds hitting the headland. However winds from 260–360° N were negatively angled due to the raised headland behind the observatory. The 30–70° N and 180–240° N zones exhibit

a small, positive tilt angle and a low drag coefficient, as might be expected for the open ocean (Kara et al., 2007; Edson et al.,

490 2013). We define these as our two air–water exchange sectors.

Author contribution

DP, TB and MY designed and set up the experiment at the Penlee Point Atmospheric Observatory. MY provided eddy covariance calculation code and DP undertook the analysis. FH and CW provided the seawater concentrations. DP prepared the manuscript with contribution from all authors.

495 Competing interests

The authors declare that they have no conflict of interest.

Acknowledgements

This work was supported by an EnvEast NERC DTP grant (NE/L002582/1). The first author would like to thank fellow authors and staff at PML for assistance in transporting equipment to the observatory. Thanks to Dr Rachael Beale (PML) for 500 her L4 time series and AMT19 data that enabled a quantitative discussion and analysis with our resolved fluxes. A further thank you to the anonymous referees who gave their time to provide helpful comments that improved the presentation and discussion of the work. Data from the Western Channel Observatory is found at <http://www.westernchannelobservatory.org.uk/>. This is contribution 10 from the Penlee Point Atmospheric Observatory.

References

505 Andreae, M. O., Ferek, R. J., Bermond, F., Byrd, K. P., Engstrom, R. T., Hardin, S., Houmere, P. D., LeMarrec, F., Raemdonck, H. and Chatfield, R. B.: Dimethyl sulfide in the marine atmosphere, *J. Geophys. Res.*, 90(D7), 12891, doi:10.1029/JD090iD07p12891, 1985.

510 Archer, S. D., Cummings, D. G., Llewellyn, C. A. and Fishwick, J. R.: Phytoplankton taxa, irradiance and nutrient availability determine the seasonal cycle of DMSP in temperate shelf seas, *Mar. Ecol. Prog. Ser.*, 394, 111–124, doi:10.3354/meps08284, 2009.

Arnold, S. R., Spracklen, D. V., Williams, J., Yassaa, N., Sciare, J., Bonsang, B., Gros, V., Peeken, I., Lewis, A. C., Alvain, S. and Moulin, C.: Evaluation of the global oceanic isoprene source and its impacts on marine organic carbon aerosol, *Atmos. Chem. Phys.*, 9(4), 1253–1262, doi:10.5194/acp-9-1253-2009, 2009.

515 Atkinson, R.: Atmospheric chemistry of VOCs and NO_x, *Atmos. Environ.*, 34(12–14), 2063–2101, doi:10.1016/S1352-2310(99)00460-4, 2000.

Atkinson, R. and Arey, J.: Atmospheric Degradation of Volatile Organic Compounds, *Chem. Rev.*, 103(12), 4605–4638, doi:10.1021/cr0206420, 2003.

Baker, A. R., Turner, S. M., Broadgate, W. J., Thompson, A., McFiggans, G. B., Vesperini, O., Nightingal, P. D., Liss, P. S. and Jickells, T. D.: Distribution and sea-air fluxes of biogenic trace gases in the eastern Atlantic Ocean, *Global Biogeochem. Cycles*, 14(3), 871–886, doi:10.1029/1999GB001219, 2000.

520 Bauer, J. E., Cai, W. J., Raymond, P. A., Bianchi, T. S., Hopkinson, C. S. and Regnier, P. A. G.: The changing carbon cycle of the coastal ocean, *Nature*, 504(7478), 61–70, doi:10.1038/nature12857, 2013.

Beale, R., Dixon, J. L., Arnold, S. R., Liss, P. S. and Nightingale, P. D.: Methanol, acetaldehyde, and acetone in the surface waters of the Atlantic Ocean, *J. Geophys. Res. Ocean.*, 118(10), 5412–5425, doi:10.1002/jgrc.20322, 2013.

525 Beale, R., Dixon, J. L., Smyth, T. J. and Nightingale, P. D.: Annual study of oxygenated volatile organic compounds in UK shelf waters, *Mar. Chem.*, 171, 96–106, doi:10.1016/j.marchem.2015.02.013, 2015.

Bell, T. G., de Bruyn, W. J., Miller, S. D., Ward, B., Christensen, K. and Saltzman, E. S.: Air-sea dimethylsulfide (DMS) gas transfer in the North Atlantic: Evidence for limited interfacial gas exchange at high wind speed, *Atmos. Chem. Phys.*, 13(21), 11073–11087, doi:10.5194/acp-13-11073-2013, 2013.

530 Bell, T. G., Landwehr, S., Miller, S. D., De Bruyn, W. J., Callaghan, A. H., Scanlon, B., Ward, B., Yang, M. and Saltzman, E. S.: Estimation of bubble-mediated air-sea gas exchange from concurrent DMS and CO₂ transfer velocities at intermediate-high wind speeds, *Atmos. Chem. Phys.*, 17(14), 9019–9033, doi:10.5194/acp-17-9019-2017, 2017.

535 Blando, J. D. and Turpin, B. J.: Secondary organic aerosol formation in cloud and fog droplets: A literature evaluation of plausibility, *Atmos. Environ.*, 34(10), 1623–1632, doi:10.1016/S1352-2310(99)00392-1, 2000.

535 Blitz, M. A., Heard, D. E., Pilling, M. J., Arnold, S. R. and Chipperfield, M. P.: Pressure and temperature-dependent quantum yields for the photodissociation of acetone between 279 and 327.5 nm, *Geophys. Res. Lett.*, 31(6), doi:10.1029/2003gl018793, 2004.

540 Blomquist, B. W., Fairall, C. W., Huebert, B. J., Kieber, D. J. and Westby, G. R.: DMS sea-air transfer velocity: Direct measurements by eddy covariance and parameterization based on the NOAA/COAREgas transfer model, *Geophys. Res. Lett.*, 33(7), 2–5, doi:10.1029/2006GL025735, 2006.

540 Blomquist, B. W., Huebert, B. J., Fairall, C. W. and Faloona, I. C.: Determining the sea-air flux of dimethylsulfide by eddy correlation using mass spectrometry, *Atmos. Meas. Tech.*, 3(1), 1–20, doi:10.5194/amt-3-1-2010, 2010.

545 Blomquist, B. W., Brumer, S. E., Fairall, C. W., Huebert, B. J., Zappa, C. J., Brooks, I. M., Yang, M., Bariteau, L., Prytherch, J., Hare, J. E., Czerski, H., Matei, A. and Pascal, R. W.: Wind Speed and Sea State Dependencies of Air-Sea Gas Transfer: Results From the High Wind Speed Gas Exchange Study (HiWinGS), *J. Geophys. Res. Ocean.*, 122(10), 8034–8062, doi:10.1002/2017JC013181, 2017.

550 Booge, D., Marandino, C. A., Schlundt, C., Palmer, P. I., Schlundt, M., Atlas, E. L., Bracher, A., Saltzman, E. S. and Wallace, D. W. R.: Can simple models predict large-scale surface ocean isoprene concentrations?, *Atmos. Chem. Phys.*, 16(18), 11807–11821, doi:10.5194/acp-16-11807-2016, 2016.

550 Booge, D., Schlundt, C., Bracher, A., Endres, S., Zäncker, B. and Marandino, C. A.: Marine isoprene production and consumption in the mixed layer of the surface ocean – a field study over two oceanic regions, *Biogeosciences*, 15(2), 649–667, doi:10.5194/bg-15-649-2018, 2018.

555 Borges, A. V., Vanderborght, J. P., Schiettecatte, L. S., Gazeau, F., Ferrón-Smith, S., Delille, B. and Frankignoulle, M.: Variability of the gas transfer velocity of CO₂ in a macrotidal estuary (the Scheldt), *Estuaries*, 27(4), 593–603, doi:10.1007/BF02907647, 2004.

555 Borges, A. V., Delille, B. and Frankignoulle, M.: Budgeting sinks and sources of CO₂ in the coastal ocean: Diversity of ecosystem counts, *Geophys. Res. Lett.*, 32(14), 1–4, doi:10.1029/2005GL023053, 2005.

Broadgate, W. J., Liss, P. S. and Penkett, S. A.: Seasonal emissions of isoprene and other reactive hydrocarbon gases from the ocean, *Geophys. Res. Lett.*, 24(21), 2675–2678, doi:10.1029/97GL02736, 1997.

560 Broadgate, W. J., Malin, G., Küpper, F. C., Thompson, A. and Liss, P. S.: Isoprene and other non-methane hydrocarbons from seaweeds: A source of reactive hydrocarbons to the atmosphere, *Mar. Chem.*, 88(1–2), 61–73, doi:10.1016/j.marchem.2004.03.002, 2004.

de Bruyn, W. J., Clark, C. D., Pagel, L. and Singh, H.: Loss rates of acetone in filtered and unfiltered coastal seawater, *Mar. Chem.*, 150, 39–44, doi:10.1016/j.marchem.2013.01.003, 2013.

565 de Bruyn, W. J., Clark, C. D., Senstad, M., Barashy, O. and Hok, S.: The biological degradation of acetaldehyde in coastal seawater, *Mar. Chem.*, 192, 13–21, doi:10.1016/j.marchem.2017.02.008, 2017.

Burkholder, J. B., Sander, S. P., Abbatt, J., Barker, J. R., Huie, R. E., Kolb, C. E., Kurylo, M. J., Orkin, V. L., Wilmouth, D. M. and Wine, P. H.: Chemical Kinetics and Photochemical Data for Use in Atmospheric Studies, Evaluation No. 18, JPL Publ. [online] Available from: <https://jpldataeval.jpl.nasa.gov/>, 2015.

570 Carslaw, N., Bell, N., Lewis, A. C., McQuaid, J. B. and Pilling, M. J.: A detailed case study of isoprene chemistry during the EASE96 Mace Head campaign, *Atmos. Environ.*, 34(18), 2827–2836, doi:10.1016/S1352-2310(00)00088-1, 2000.

Charlson, R. J., Lovelock, J. E., Andreae, M. O. and Warren, S. G.: Oceanic phytoplankton, atmospheric sulphur, cloud albedo and climate, *Nature*, 326(6114), 655–661, doi:10.1038/326655a0, 1987.

575 Ciuraru, R., Fine, L., Pinxteren, M. Van, D'Anna, B., Herrmann, H. and George, C.: Unravelling New Processes at Interfaces: Photochemical Isoprene Production at the Sea Surface, *Environ. Sci. Technol.*, 49(22), 13199–13205, doi:10.1021/acs.est.5b02388, 2015.

Cloern, J. E., Foster, S. Q. and Kleckner, A. E.: Phytoplankton primary production in the world's estuarine-coastal ecosystems, *Biogeosciences*, 11(9), 2477–2501, doi:10.5194/bg-11-2477-2014, 2014.

Dani, K. G. S. and Loreto, F.: Trade-Off Between Dimethyl Sulfide and Isoprene Emissions from Marine Phytoplankton, *Trends Plant Sci.*, 22(5), 361–372, doi:10.1016/j.tplants.2017.01.006, 2017.

580 Dixon, J. L., Beale, R. and Nightingale, P. D.: Production of methanol, acetaldehyde, and acetone in the Atlantic Ocean, *Geophys. Res. Lett.*, 40(17), 4700–4705, doi:10.1002/grl.50922, 2013.

Dixon, J. L., Beale, R., Sargeant, S. L., Tarran, G. A. and Nightingale, P. D.: Microbial acetone oxidation in coastal seawater, *Front. Microbiol.*, 5(MAY), 1–9, doi:10.3389/fmicb.2014.00243, 2014.

585 Edson, J. B., Jampana, V., Weller, R. A., Bigorre, S. P., Plueddemann, A. J., Fairall, C. W., Miller, S. D., Mahrt, L., Vickers, D. and Hersbach, H.: On the exchange of momentum over the open ocean, *J. Phys. Oceanogr.*, 43(8), 1589–1610, doi:10.1175/JPO-D-12-0173.1, 2013.

590 Exton, D. A., Suggett, D. J., McGenity, T. J. and Steinke, M.: Chlorophyll-normalized isoprene production in laboratory cultures of marine microalgae and implications for global models, *Limnol. Oceanogr.*, 58(4), 1301–1311, doi:10.4319/lo.2013.58.4.1301, 2013.

Fischer, E. V., Jacob, D. J., Millet, D. B., Yantosca, R. M. and Mao, J.: The role of the ocean in the global atmospheric budget of acetone, *Geophys. Res. Lett.*, 39(1), 3–7, doi:10.1029/2011GL050086, 2012.

595 Guenther, A. B., Karl, T. R., Harley, P., Wiedinmyer, C., Palmer, P. I. and Geron, C.: Estimates of global terrestrial isoprene emissions using MEGAN (Model of Emissions of Gases and Aerosols from Nature), *Atmos. Chem. Phys.*, 6(11), 3181–3210, doi:10.5194/acp-6-3181-2006, 2006.

Hackenberg, S. C., Andrews, S. J., Airs, R., Arnold, S. R., Bouman, H. A., Brewin, R. J. W., Chance, R. J., Cummings, D., Dall’Olmo, G., Lewis, A. C., Minaeian, J. K., Reifel, K. M., Small, A., Tarran, G. A., Tilstone, G. H. and Carpenter, L. J.: Potential controls of isoprene in the surface ocean, *Global Biogeochem. Cycles*, 31(4), 644–662, doi:10.1002/2016GB005531, 2017.

600 Halsey, K. H., Giovannoni, S. J., Graus, M., Zhao, Y., Landry, Z., Thrash, J. C., Vergin, K. L. and De Gouw, J. A.: Biological cycling of volatile organic carbon by phytoplankton and bacterioplankton, *Limnol. Oceanogr.*, 62(6), 2650–2661, doi:10.1002/lno.10596, 2017.

605 Heald, C. L., Goldstein, A. H., Allan, J. D., Aiken, A. C., Apel, E. C., Atlas, E. L., Baker, A. K., Bates, T. S., Beyersdorf, A. J., Blake, D. R., Campos, T., Coe, H., Crounse, J. D., DeCarlo, P. F., De Gouw, J. A., Dunlea, E. J., Flocke, F. M., Fried, A., Goldan, P. D., Griffin, R. J., Herndon, S. C., Holloway, J. S., Holzinger, R., Jimenez, J. L., Junkermann, W., Kuster, W. C., Lewis, A. C., Meinardi, S., Millet, D. B., Onasch, T., Polidori, A., Quinn, P. K., Riemer, D. D., Roberts, J. M., Salcedo, D., Sive, B., Swanson, A. L., Talbot, R., Warneke, C., Weber, R. J., Weibring, P., Wennberg, P. O., Worsnop, D. R., Wittig, A. E., Zhang, R., Zheng, J. and Zheng, W.: Total observed organic carbon (TOOC) in the atmosphere: A synthesis of North American observations, *Atmos. Chem. Phys.*, 8(7), 2007–2025, doi:10.5194/acp-8-2007-2008, 2008.

610 Henze, D. K. and Seinfeld, J. H.: Global secondary organic aerosol from isoprene oxidation, *Geophys. Res. Lett.*, 33(9), 6–9, doi:10.1029/2006GL025976, 2006.

Hopkins, F. E. and Archer, S. D.: Consistent increase in dimethyl sulfide (DMS) in response to high CO₂ in five shipboard bioassays from contrasting NW European waters, *Biogeosciences*, 11(18), 4925–4940, doi:10.5194/bg-11-4925-2014, 2014.

615 Horowitz, L. W., Walters, S., Mauzerall, D. L., Emmons, L. K., Rasch, P. J., Granier, C., Tie, X., Lamarque, J. F., Schultz, M. G., Tyndall, G. S., Orlando, J. J. and Brasseur, G. P.: A global simulation of tropospheric ozone and related tracers: Description and evaluation of MOZART, version 2, *J. Geophys. Res. Atmos.*, 108(24), doi:10.1029/2002jd002853, 2003.

Huebert, B. J., Blomquist, B. W., Yang, M., Archer, S. D., Nightingale, P. D., Yelland, M. J., Stephens, J., Pascal, R. W. and Moat, B. I.: Linearity of DMS transfer coefficient with both friction velocity and wind speed in the moderate wind speed range, *Geophys. Res. Lett.*, 37(1), 0–4, doi:10.1029/2009GL041203, 2010.

620 Hyson, P., Garratt, J. R. and Francey, R. J.: Algebraic and Electronic Corrections of Measured uw Covariance in the Lower Atmosphere, *J. Appl. Meteorol.*, 16(1), 43–47, doi:10.1175/1520-0450(1977)016<0043:AAECOM>2.0.CO;2, 1977.

Jacob, D. J., Field, B. D., Jin, E. M., Bey, I., Li, Q., Logan, J. A., Yantosca, R. M. and Singh, H. B.: Atmospheric budget of acetone, *J. Geophys. Res. Atmos.*, 107(D10), doi:10.1029/2001JD000694, 2002.

625 Johnson, M. T.: A numerical scheme to calculate temperature and salinity dependent air-water transfer velocities for any gas, *Ocean Sci.*, 6(4), 913–932, doi:10.5194/os-6-913-2010, 2010.

Kaimal, J., Wyngaard, J., Izumi, Y. and Cote, O.: Spectral characteristics of surface-layer turbulence, *Q. J. R. Meteorol. Soc.*, 98(417), 563–589, doi:10.1256/smsqj.41706, 1972.

Kara, A. B., Metzger, E. J. and Bourassa, M. A.: Ocean current and wave effects on wind stress drag coefficient over the global ocean, *Geophys. Res. Lett.*, 34(1), 2–5, doi:10.1029/2006GL027849, 2007.

630 Kesselmeier, J. and Staudt, M.: Biogenic Volatile Organic Compound (VOC): An Overview on Emissions, Physiology and Ecology, *J. Atmos. Chem.*, 33(1), 23–88, doi:10.1023/A:1006127516791, 1999.

Khan, M. A. H., Cooke, M. C., Utetbe, S. R., Archibald, A. T., Maxwell, P., Morris, W. C., Xiao, P., Derwent, R. G., Jenkin, M. E., Percival, C. J., Walsh, R. C., Young, T. D. S., Simmonds, P. G., Nickless, G., O’Doherty, S. and Shallcross, D. E.: A study of global atmospheric budget and distribution of acetone using global atmospheric model STOCHEM-CRI, *Atmos. Environ.*, 112, 269–277, doi:10.1016/j.atmosenv.2015.04.056, 2015.

Kieber, R. J., Zhou, X. and Mopper, K.: Formation of carbonyl compounds from UV-induced photodegradation of humic substances in natural waters: Fate of riverine carbon in the sea, *Limnol. Oceanogr.*, 35(7), 1503–1515,

640 Kiene, R. P., Linn, L. J. and Bruton, J. A.: New and important roles for DMSP in marine microbial communities, *J. Sea Res.*, 43(3–4), 209–224, doi:10.1016/S1385-1101(00)00023-X, 2000.

Kim, M. J., Novak, G. A., Zoerb, M. C., Yang, M., Blomquist, B. W., Huebert, B. J., Cappa, C. D. and Bertram, T. H.: Air-Sea exchange of biogenic volatile organic compounds and the impact on aerosol particle size distributions, *Geophys. Res. Lett.*, 44(8), 3887–3896, doi:10.1002/2017GL072975, 2017.

645 Lana, A., Bell, T. G., Simó, R., Vallina, S. M., Ballabrera-Poy, J., Kettle, A. J., Dachs, J., Bopp, L., Saltzman, E. S., Stefels, J., Johnson, J. E. and Liss, P. S.: An updated climatology of surface dimethylsulfide concentrations and emission fluxes in the global ocean, *Global Biogeochem. Cycles*, 25(1), 1–17, doi:10.1029/2010GB003850, 2011.

Lewis, A. C., Carpenter, L. J. and Pilling, M. J.: Nonmethane hydrocarbons in Southern Ocean boundary layer air, *J. Geophys. Res. Atmos.*, 106(D5), 4987–4994, doi:10.1029/2000JD900634, 2001.

650 Lewis, A. C., Hopkins, J. R., Carpenter, L. J., Stanton, J., Read, K. A. and Pilling, M. J.: Sources and sinks of acetone, methanol, and acetaldehyde in North Atlantic marine air, *Atmos. Chem. Phys.*, 5(7), 1963–1974, doi:10.5194/acp-5-1963-2005, 2005.

Li, M., Karu, E., Brenninkmeijer, C. A. M., Fischer, H., Lelieveld, J. and Williams, J.: Tropospheric OH and stratospheric OH and Cl concentrations determined from CH₄, CH₃Cl, and SF₆ measurements, *Clim. Atmos. Sci.*, 1(1), 29, doi:10.1038/s41612-018-0041-9, 2018.

655 Liss, P. S. and Slater, P. G.: Flux of Gases across the Air-Sea Interface, *Nature*, 247(5438), 181–184, doi:10.1038/247181a0, 1974.

Loades, D. C., Yang, M., Bell, T. G., Vaughan, A. R., Pound, R. J., Metzger, S., Lee, J. D. and Carpenter, L. J.: Ozone deposition to a coastal sea: comparison of eddy covariance observations with reactive air–sea exchange models, *Atmos. Meas. Tech.*, 13(12), 6915–6931, doi:10.5194/amt-13-6915-2020, 2020.

660 Mackay, D. and Yeun, A. T. K.: Mass Transfer Coefficient Correlations for Volatilization of Organic Solutes from Water, *Environ. Sci. Technol.*, 17(4), 211–217, doi:10.1021/es00110a006, 1983.

Marandino, C. A., de Bruyn, W. J., Miller, S. D., Prather, M. J. and Saltzman, E. S.: Oceanic uptake and the global atmospheric acetone budget, *Geophys. Res. Lett.*, 32(15), doi:10.1029/2005GL023285, 2005.

665 Millet, D. B., Guenther, A. B., Siegel, D. A., Nelson, N. B., Singh, H. B., De Gouw, J. A., Warneke, C., Williams, J., Eerdekens, G., Sinha, V., Karl, T. R., Flocke, F., Apel, E. C., Riemer, D. D., Palmer, P. I. and Barkley, M.: Global atmospheric budget of acetaldehyde: 3-D model analysis and constraints from in-situ and satellite observations, *Atmos. Chem. Phys.*, 10(7), 3405–3425, doi:10.5194/acp-10-3405-2010, 2010.

Moore, R. M., Oram, D. E. and Penkett, S. A.: Production of isoprene by marine phytoplankton cultures, *Geophys. Res. Lett.*, 21(23), 2507–2510, doi:10.1029/94GL02363, 1994.

670 Nightingale, P. D., Malin, G., Law, C. S., Watson, A. J., Liss, P. S., Liddicoat, M. I., Boutin, J. and Upstill-Goddard, R. C.: In situ evaluation of air-sea gas exchange parameterizations using novel conservative and volatile tracers, *Global Biogeochem. Cycles*, 14(1), 373–387, doi:10.1029/1999GB900091, 2000.

Palmer, P. I. and Shaw, S. L.: Quantifying global marine isoprene fluxes using MODIS chlorophyll observations, *Geophys. Res. Lett.*, 32(9), 1–5, doi:10.1029/2005GL022592, 2005.

675 Quinn, P. K., Bates, T. S., Coffman, D. J., Upchurch, L., Johnson, J. E., Moore, R., Ziemb, L., Bell, T. G., Saltzman, E. S., Graff, J. and Behrenfeld, M. J.: Seasonal Variations in Western North Atlantic Remote Marine Aerosol Properties, *J. Geophys. Res. Atmos.*, 124(24), 14240–14261, doi:10.1029/2019JD031740, 2019.

Rolph, G., Stein, A. and Stunder, B.: Real-time Environmental Applications and Display sYstem: READY, *Environ. Model. Softw.*, 95, 210–228, doi:10.1016/j.envsoft.2017.06.025, 2017.

680 Royer, S. J., Galí, M., Mahajan, A. S., Ross, O. N., Pérez, G. L., Saltzman, E. S. and Simó, R.: A high-resolution time-depth view of dimethylsulphide cycling in the surface sea, *Sci. Rep.*, 6(November 2015), 1–13, doi:10.1038/srep32325, 2016.

Saltzman, E. S., King, D. B., Holmen, K. and Leck, C.: Experimental determination of the diffusion coefficient of dimethylsulfide in water, *J. Geophys. Res.*, 98(C9), 481–486, doi:10.1029/93jc01858, 1993.

685 Sander, R.: Compilation of Henry's law constants (version 4.0) for water as solvent, *Atmos. Chem. Phys.*, 15(8), 4399–4981, doi:10.5194/acp-15-4399-2015, 2015.

Schlundt, C., Tegtmeier, S., Lennartz, S. T., Bracher, A., Cheah, W., Krüger, K., Quack, B. and Marandino, C. A.: Oxygenated volatile organic carbon in the western Pacific convective center: Ocean cycling, air-sea gas exchange and atmospheric transport, *Atmos. Chem. Phys.*, 17(17), 10837–10854, doi:10.5194/acp-17-10837-2017, 2017.

690 Schwarz, K., Filipiak, W. and Amann, A.: Determining concentration patterns of volatile compounds in exhaled breath by PTR-MS, *J. Breath Res.*, 3(2), 027002, doi:10.1088/1752-7155/3/2/027002, 2009.

Shaw, S. L., Chisholm, S. W. and Prinn, R. G.: Isoprene production by Prochlorococcus, a marine cyanobacterium, and other phytoplankton, *Mar. Chem.*, 80(4), 227–245, doi:10.1016/S0304-4203(02)00101-9, 2003.

Spirig, C., Neftel, A., Ammann, C., Dommen, J., Grabmer, W., Thielmann, A., Schaub, A., Beauchamp, J. L., Wisthaler, A. and Hansel, A.: Eddy covariance flux measurements of biogenic VOCs during ECHO 2003 using proton transfer reaction mass spectrometry, *Atmos. Chem. Phys.*, 5(2), 465–481, doi:10.5194/acp-5-465-2005, 2005.

Stein, A. F., Draxler, R. R., Rolph, G. D., Stunder, B. J. B., Cohen, M. D. and Ngan, F.: NOAA's Hysplit atmospheric transport and dispersion modeling system, *Bull. Am. Meteorol. Soc.*, 96(12), 2059–2077, doi:10.1175/BAMS-D-14-00110.1, 2015.

Tanner, C. B. and Thurtell, G. W.: Anemoclinometer measurements of Reynolds stress and heat transport in the atmospheric surface layer., 1969.

Uncles, R. J., Stephens, J. A. and Harris, C.: Physical processes in a coupled bay-estuary coastal system: Whitsand Bay and Plymouth Sound, *Prog. Oceanogr.*, 137, 360–384, doi:10.1016/j.pocean.2015.04.019, 2015.

Upstill-Goddard, R. C.: Air-sea gas exchange in the coastal zone, *Estuar. Coast. Shelf Sci.*, 70(3), 388–404, doi:10.1016/j.ecss.2006.05.043, 2006.

Veres, P. R., Andrew Neuman, J., Bertram, T. H., Assaf, E., Wolfe, G. M., Williamson, C. J., Weinzierl, B., Tilmes, S., Thompson, C. R., Thames, A. B., Schroder, J. C., Saiz-Lopez, A., Rollins, A. W., Roberts, J. M., Price, D., Peischl, J., Nault, B. A., Møller, K. H., Miller, D. O., Meinardi, S., Li, Q., Lamarque, J. F., Kupc, A., Kjaergaard, H. G., Kinnison, D., Jimenez, J. L., Jernigan, C. M., Hornbrook, R. S., Hills, A., Dollner, M., Day, D. A., Cuevas, C. A., Campuzano-Jost, P., Burkholder, J. B., Paul Bui, T., Brune, W. H., Brown, S. S., Brock, C. A., Bourgeois, I., Blake, D. R., Apel, E. C. and Ryerson, T. B.: Global airborne sampling reveals a previously unobserved dimethyl sulfide oxidation mechanism in the marine atmosphere, *Proc. Natl. Acad. Sci. U. S. A.*, 117(9), 4505–4510, doi:10.1073/pnas.1919344117, 2020.

Wang, S., Hornbrook, R. S., Hills, A., Emmons, L. K., Tilmes, S., Lamarque, J. F., Jimenez, J. L., Campuzano-Jost, P., Nault, B. A., Crounse, J. D., Wennberg, P. O., Kim, M., Allen, H. M., Ryerson, T. B., Thompson, C. R., Peischl, J., Moore, F., Nance, D., Hall, B., Elkins, J., Tanner, D., Huey, L. G., Hall, S. R., Ullmann, K., Orlando, J. J., Tyndall, G. S., Flocke, F. M., Ray, E., Hanisco, T. F., Wolfe, G. M., St. Clair, J., Commane, R., Daube, B., Barletta, B., Blake, D. R., Weinzierl, B., Dollner, M., Conley, A., Vitt, F., Wofsy, S. C., Riemer, D. D. and Apel, E. C.: Atmospheric Acetaldehyde: Importance of Air-Sea Exchange and a Missing Source in the Remote Troposphere, *Geophys. Res. Lett.*, 46(10), 5601–5613, doi:10.1029/2019GL082034, 2019.

Wang, S., Apel, E. C., Schwantes, R., Bates, K., Jacob, D., Fischer, E., Hornbrook, R. S., Hills, A., Emmons, L., Pan, L., Honomichl, S., Tilmes, S., Lamarque, J., Yang, M., Marandino, C., Saltzman, E., Bruyn, W., Kameyama, S., Tanimoto, H., Omori, Y., Hall, S., Ullmann, K., Ryerson, T., Thompson, C., Peischl, J., Daube, B., Commane, R., McKain, K., Sweeney, C., Thames, A., Miller, D., Brune, W. H., Diskin, G., DiGangi, J. and Wofsy, S.: Global Atmospheric Budget of Acetone: Air-Sea Exchange and the Contribution to Hydroxyl Radicals, *J. Geophys. Res. Atmos.*, 2, 1–23, doi:10.1029/2020JD032553, 2020a.

Wang, W.-L., Song, G., Primeau, F., Saltzman, E., Bell, T. G. and Moore, J. K.: Global ocean dimethyl sulfide climatology estimated from observations and an artificial neural network, *Biogeosciences Discuss.*, 1–26, doi:10.1002/essoar.10502127.1, 2020b.

Warneck, P. and Moortgat, G. K.: Quantum yields and photodissociation coefficients of acetaldehyde in the troposphere, *Atmos. Environ.*, 62, 153–163, doi:10.1016/j.atmosenv.2012.08.024, 2012.

Warneke, C., De Gouw, J. A., Kuster, W. C., Goldan, P. D. and Fall, R.: Validation of atmospheric VOC measurements by proton-transfer-reaction mass spectrometry using a gas-chromatographic preseparation method, *Environ. Sci. Technol.*, 37(11), 2494–2501, doi:10.1021/es0262661, 2003.

Williams, J., Holzinger, R., Gros, V., Xu, X., Atlas, E. L. and Wallace, D. W. R.: Measurements of organic species in air and seawater from the tropical Atlantic, *Geophys. Res. Lett.*, 31(23), 1–5, doi:10.1029/2004GL020012, 2004.

Wofsy, S. C., Afshar, S., Allen, H. M., Apel, E. C., Asher, E. C., Barletta, B., Bent, J., Bian, H., Biggs, B. C., Blake, D. R., Blake, N., Bourgeois, I., Brock, C. A., Brune, W. H., Budney, J. W., Bui, T. P., Butler, A., Campuzano-Jost, P., Chang, C. S., Chin, M., Commane, R., Correa, G., Crounse, J. D., Cullis, P. D., Daube, B. C., Day, D. A., Dean-Day, J. M., Dibb, J. E., DiGangi, J. P., Diskin, G. S., Dollner, M., Elkins, J. W., Erdesz, F., Fiore, A. M., Flynn, C. M., Froyd, K. D., Gesler, D. W., Hall, S. R., Hanisco, T. F., Hannun, R. A., Hills, A. J., Hints, E. J., Hoffman, A., Hornbrook, R. S., Huey, L. G., Hughes, S., Jimenez, J. L., Johnson, B. J., Katich, J. M., Keeling, R. F., Kim, M. J., Kupc, A., Lait, L. R., Lamarque, J.-F., Liu, J., McKain, K., McLaughlin, R. J., Meinardi, S., Miller, D. O., Montzka, S. A., Moore, F. L., Morgan, E. J., Murphy, D. M., Murray, L. T., Nault, B. A., Neuman, J. A., Newman, P. A., Nicely, J. M., Pan, X., Paplawsky, W., Peischl, J., Prather, M. J., Price, D. J., Ray, E. A., Reeves, J. M., Richardson, M., Rollins, A. W., Rosenlof, K. H., Ryerson, T. B., Scheuer, E., Schill, G. P., Schroder, J. C., Schwarz, J. P., St. Clair, J. M., Steenrod, S. D., Stephens, B. B., Strode, S. A., Sweeney, C., Tanner, D., Teng, A. P., Thames, A. B., Thompson, C. R., Ullmann, K., Veres, P. R., Vieznor, N., Wagner, N. L., Watt, A., Weber, R., Weinzierl, B., et al.: ATom: Merged Atmospheric Chemistry, Trace Gases, and Aerosols, doi:10.3334/ORNLDAA/1581, 2018.

Wohl, C., Capelle, D., Jones, A., Sturges, W. T., Nightingale, P. D., Else, B. G. T. and Yang, M.: Segmented flow coil equilibrator coupled to a proton-transfer-reaction mass spectrometer for measurements of a broad range of volatile organic

compounds in seawater, *Ocean Sci.*, 15(4), 925–940, doi:10.5194/os-15-925-2019, 2019.

750 Wohl, C., Brown, I. J., Kitidis, V., Jones, A. E., Sturges, W. T., Nightingale, P. D. and Yang, M.: Underway seawater and atmospheric measurements of volatile organic compounds in the Southern Ocean, *Biogeosciences*, 17(9), 2593–2619, doi:10.5194/bg-17-2593-2020, 2020.

Yang, M. and Fleming, Z. L.: Estimation of atmospheric total organic carbon (TOC) - Paving the path towards carbon budget closure, *Atmos. Chem. Phys.*, 19(1), 459–471, doi:10.5194/acp-19-459-2019, 2019.

755 Yang, M., Blomquist, B. W., Fairall, C. W., Archer, S. D. and Huebert, B. J.: Air-sea exchange of dimethylsulfide in the Southern Ocean: Measurements from so GasEx compared to temperate and tropical regions, *J. Geophys. Res. Ocean.*, 116(8), 1–17, doi:10.1029/2010JC006526, 2011a.

760 Yang, M., Huebert, B. J., Blomquist, B. W., Howell, S. G., Shank, L. M., McNaughton, C. S., Clarke, A. D., Hawkins, L. N., Russell, L. M., Covert, D. S., Coffman, D. J., Bates, T. S., Quinn, P. K., Zagorac, N., Bandy, A. R., de Szoek, S. P., Zuidema, P. D., Tucker, S. C., Brewer, W. A., Benedict, K. B. and Collett, J. L.: Atmospheric sulfur cycling in the southeastern Pacific – longitudinal distribution, vertical profile, and diel variability observed during VOCALS-REx, *Atmos. Chem. Phys.*, 11(10), 5079–5097, doi:10.5194/acp-11-5079-2011, 2011b.

Yang, M., Nightingale, P. D., Beale, R., Liss, P. S., Blomquist, B. W. and Fairall, C. W.: Atmospheric deposition of methanol over the Atlantic Ocean, *Proc. Natl. Acad. Sci.*, 110(50), 20034–20039, doi:10.1073/pnas.1317840110, 2013a.

765 Yang, M., Archer, S. D., Blomquist, B. W., Ho, D. T., Lance, V. P. and Torres, R. J.: Lagrangian evolution of DMS during the Southern Ocean gas exchange experiment: The effects of vertical mixing and biological community shift, *J. Geophys. Res. Ocean.*, 118(12), 6774–6790, doi:10.1002/2013JC009329, 2013b.

Yang, M., Beale, R., Smyth, T. J. and Blomquist, B. W.: Measurements of OVOC fluxes by eddy covariance using a proton-transfer- reaction mass spectrometer - method development at a coastal site, *Atmos. Chem. Phys.*, 13(13), 6165–6184, doi:10.5194/acp-13-6165-2013, 2013c.

770 Yang, M., Blomquist, B. W. and Nightingale, P. D.: Air-sea exchange of methanol and acetone during HiWinGS: Estimation of air phase, water phase gas transfer velocities, *J. Geophys. Res. Ocean.*, 119(10), 7308–7323, doi:10.1002/2014JC010227, 2014a.

775 Yang, M., Beale, R., Liss, P. S., Johnson, M. T., Blomquist, B. W. and Nightingale, P. D.: Air-sea fluxes of oxygenated volatile organic compounds across the Atlantic Ocean, *Atmos. Chem. Phys.*, 14(14), 7499–7517, doi:10.5194/acp-14-7499-2014, 2014b.

Yang, M., Bell, T. G., Hopkins, F. E., Kitidis, V., Cazenave, P. W., Nightingale, P. D., Yelland, M. J., Pascal, R. W., Prytherch, J., Brooks, I. M. and Smyth, T. J.: Air-sea fluxes of CO₂ and CH₄ from the penlee point atmospheric observatory on the south-west coast of the UK, *Atmos. Chem. Phys.*, 16(9), 5745–5761, doi:10.5194/acp-16-5745-2016, 2016a.

780 Yang, M., Bell, T. G., Blomquist, B. W., Fairall, C. W., Brooks, I. M. and Nightingale, P. D.: Air-sea transfer of gas phase controlled compounds, *IOP Conf. Ser. Earth Environ. Sci.*, 35(1), doi:10.1088/1755-1315/35/1/012011, 2016b.

Yang, M., Bell, T. G., Hopkins, F. E. and Smyth, T. J.: Attribution of atmospheric sulfur dioxide over the English Channel to dimethyl sulfide and changing ship emissions, *Atmos. Chem. Phys.*, 16(8), 4771–4783, doi:10.5194/acp-16-4771-2016, 2016c.

785 Yang, M., Prytherch, J., Kozlova, E., Yelland, M. J., Parenkat Mony, D. and Bell, T. G.: Comparison of two closed-path cavity-based spectrometers for measuring air-water CO₂ and CH₄ fluxes by eddy covariance, *Atmos. Meas. Tech.*, 9(11), 5509–5522, doi:10.5194/amt-9-5509-2016, 2016d.

Yang, M., Bell, T. G., Brown, I. J., Fishwick, J. R., Kitidis, V., Nightingale, P. D., Rees, A. P. and Smyth, T. J.: Insights from year-long measurements of air–water CH₄ and CO₂ exchange in a coastal environment, *Biogeosciences*, 16(5), 961–978, doi:10.5194/bg-16-961-2019, 2019a.

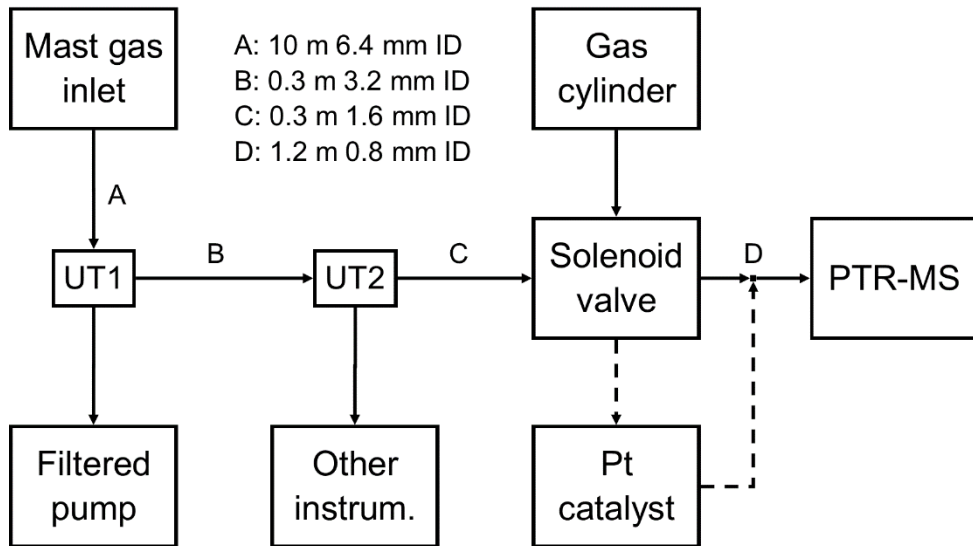
790 Yang, M., Norris, S. J., Bell, T. G. and Brooks, I. M.: Sea spray fluxes from the southwest coast of the United Kingdom-Dependence on wind speed and wave height, *Atmos. Chem. Phys.*, 19(24), 15271–15284, doi:10.5194/acp-19-15271-2019, 2019b.

Zhou, S., Gonzalez, L., Leithead, A., Finewax, Z., Thalman, R., Vlasenko, A., Vagle, S., Miller, L. A., Li, S. M., Bureekul, S., Furutani, H., Uematsu, M., Volkamer, R. and Abbott, J. P. D.: Formation of gas-phase carbonyls from heterogeneous oxidation of polyunsaturated fatty acids at the air-water interface and of the sea surface microlayer, *Atmos. Chem. Phys.*, 14(3), 1371–1384, doi:10.5194/acp-14-1371-2014, 2014.

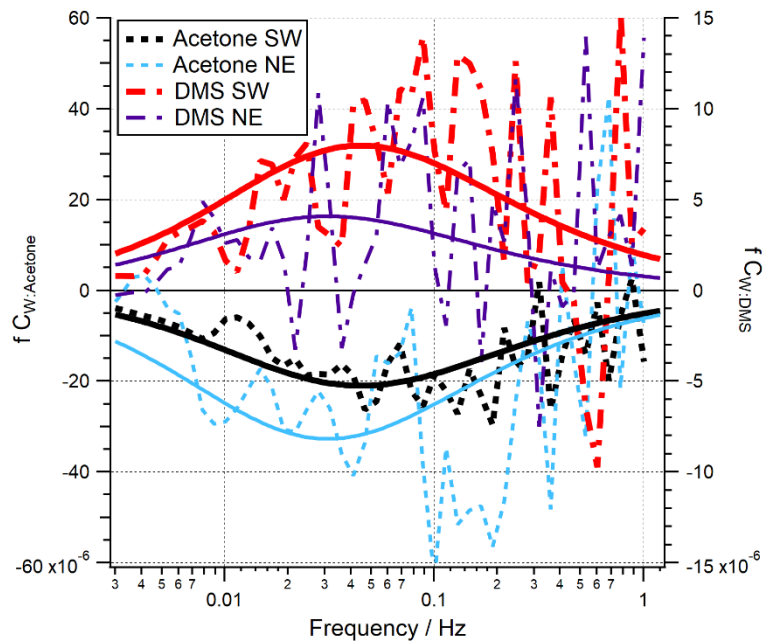
Zhou, X. and Mopper, K.: Photochemical production of low-molecular-weight carbonyl compounds in seawater and surface microlayer and their air-sea exchange, *Mar. Chem.*, 56(3–4), 201–213, doi:10.1016/S0304-4203(96)00076-X, 1997.

800 Zhu, Y. and Kieber, D. J.: Wavelength- and Temperature-Dependent Apparent Quantum Yields for Photochemical Production of Carbonyl Compounds in the North Pacific Ocean, *Environ. Sci. Technol.*, 52(4), 1929–1939, doi:10.1021/acs.est.7b05462, 2018.

Figures & tables



805 **Figure 1:** Schematic of the tubing set-up used to draw atmospheric sample to the gas instrument (PTR-MS). Dashed lines represent the set-up of the platinum catalyst before the synthetic gas blank was added. UT represents union-tee; a three-way static connection.



810 **Figure 2:** Mean flux spectra for acetone and DMS in the SW and NE wind sectors. Dashed/broken lines represent PPAO observations. Solid lines represent the idealised spectral fits (Kaimal et al., 1972), where measurement height and wind speed are specified according to the measurement conditions.

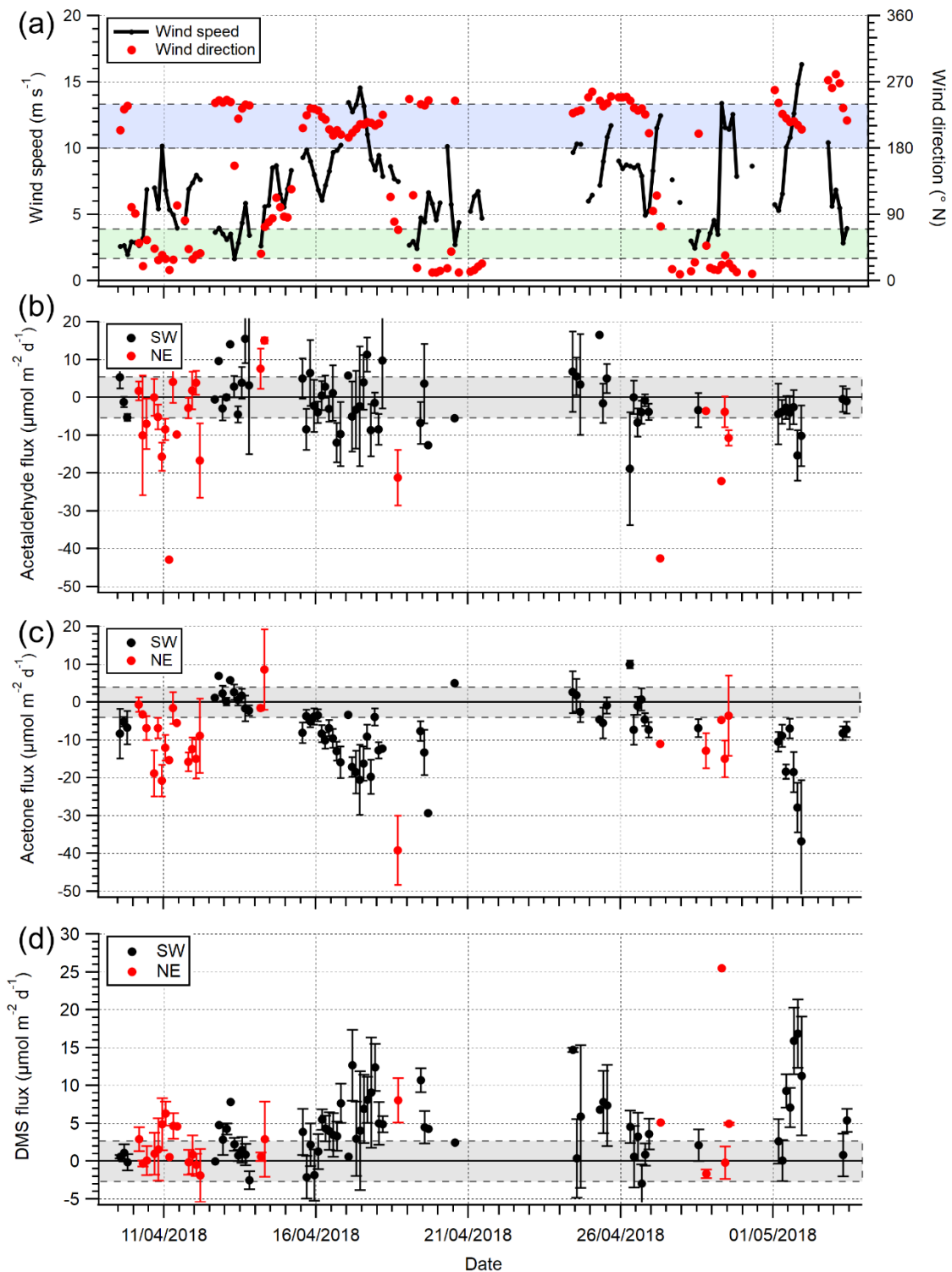


Figure 3: Time series of 3 h averages of a) wind speed (U_{10}) and wind direction, b) acetaldehyde flux, c) acetone flux and d) DMS fluxes for the open water (180–240° N) and Plymouth Sound (30–70° N) wind sectors that met quality control criteria. Error bars are 1 standard error. The blue and green shaded zone in a subplot a represent the two wind sectors. The grey shaded zones in subplots b–d represent limits of detection for 3 h averages; 5.8, 4.0 and 2.7 $\mu\text{mol m}^{-2} \text{d}^{-1}$ for acetaldehyde, acetone, DMS respectively.

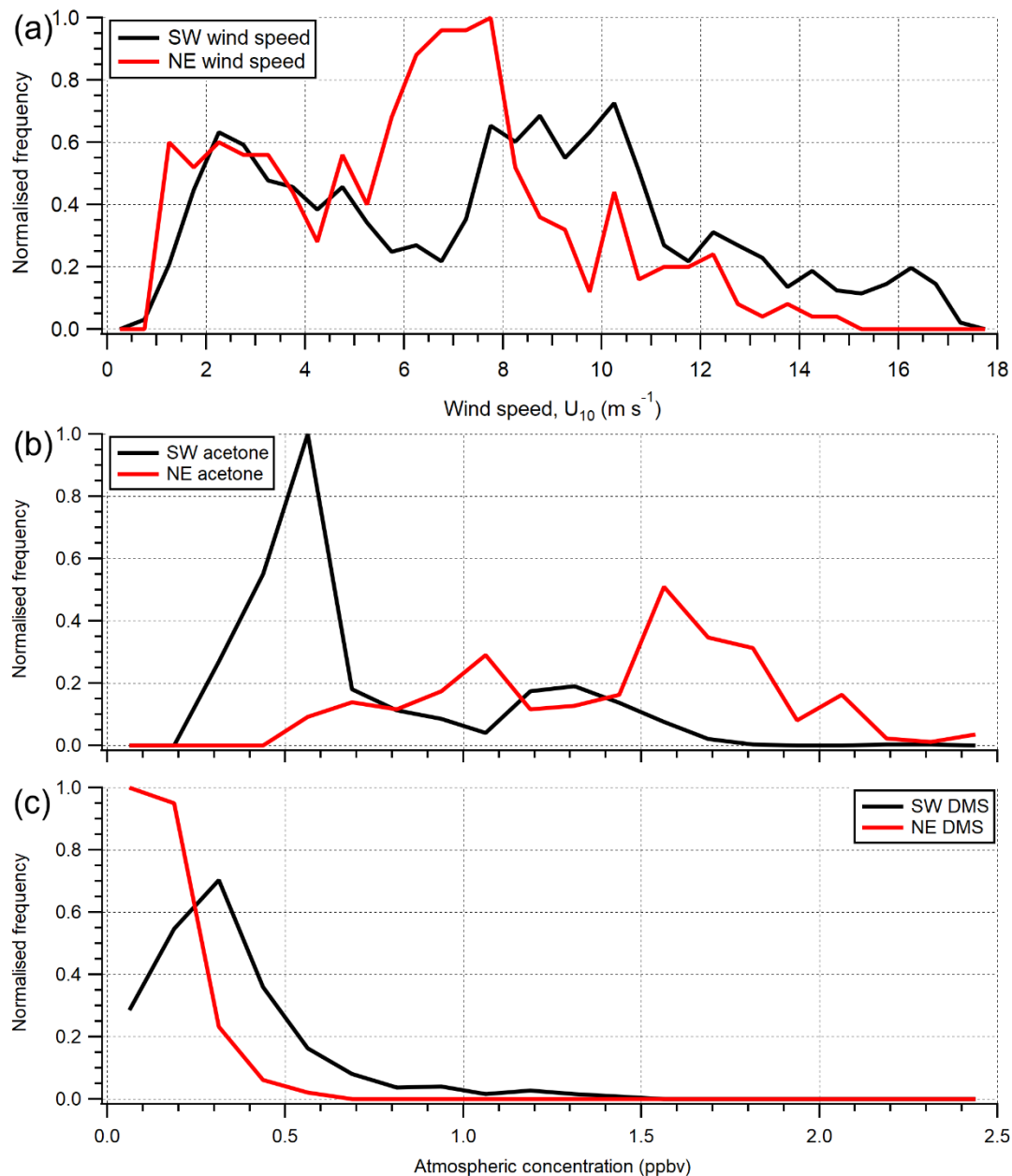


Figure 4: Histogram of a) wind speed (U_{10}) and b) acetone and c) DMS atmospheric gas phase mixing ratio over the entire campaign. Histograms are normalised for probability density separately and then to the same relative maximum occurrence. The gas mixing ratio calculations here use extrapolated blanks here, which introduce some uncertainty, however the two wind sectors can still be compared.

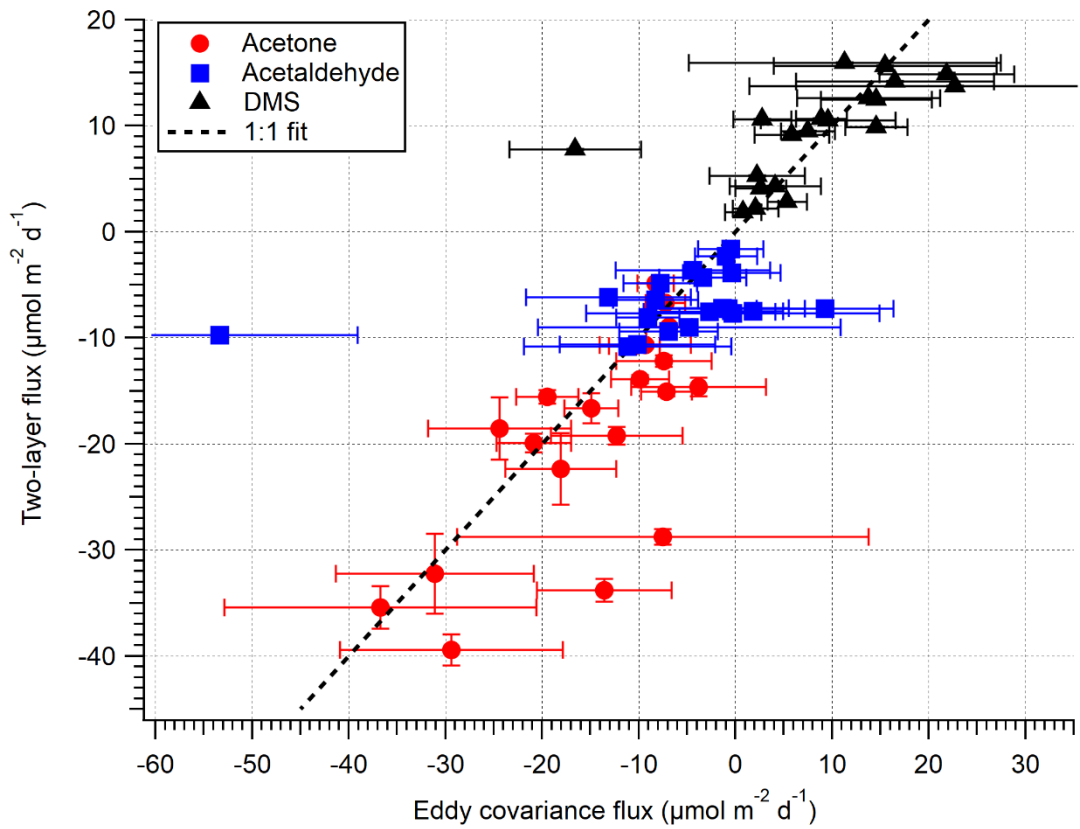
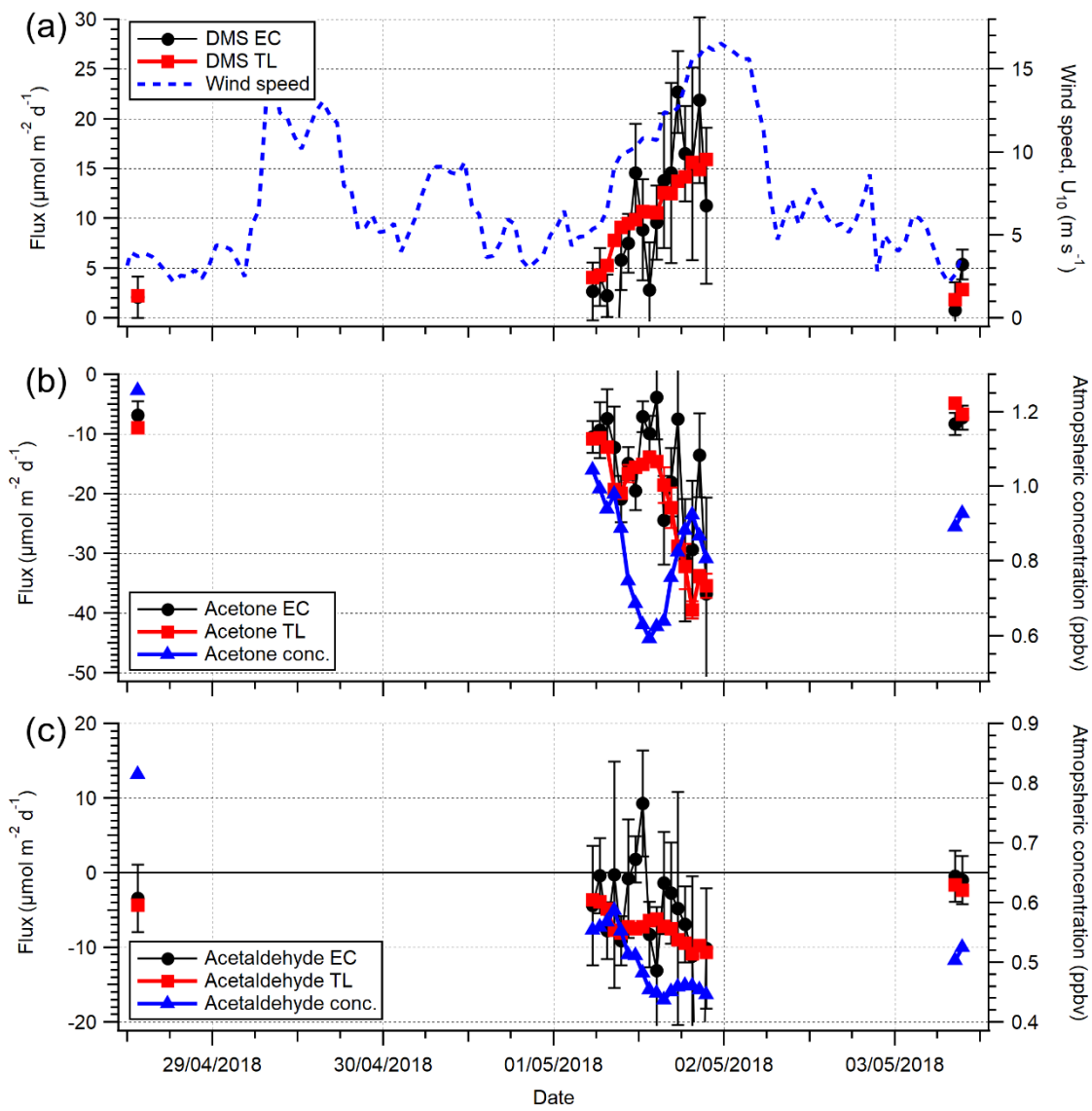


Figure 5: A comparison between EC and bulk TL fluxes (hourly) for the open water sector during the dates (27/04/18–03/05/18). The error on EC measurements is one SE, whilst the error on TL is the propagated error of one SD in concentration and solubility.



825

Figure 6: A comparison between a) DMS, b) acetone and c) acetaldehyde EC and TL fluxes (hourly) for the open water sector during the dates 27/04/18–03/05/18. Wind speed (U_{10}) is provided in a). The error on EC measurements is one SE, whilst the error on TL is the propagated error of one SD in concentration and solubility.

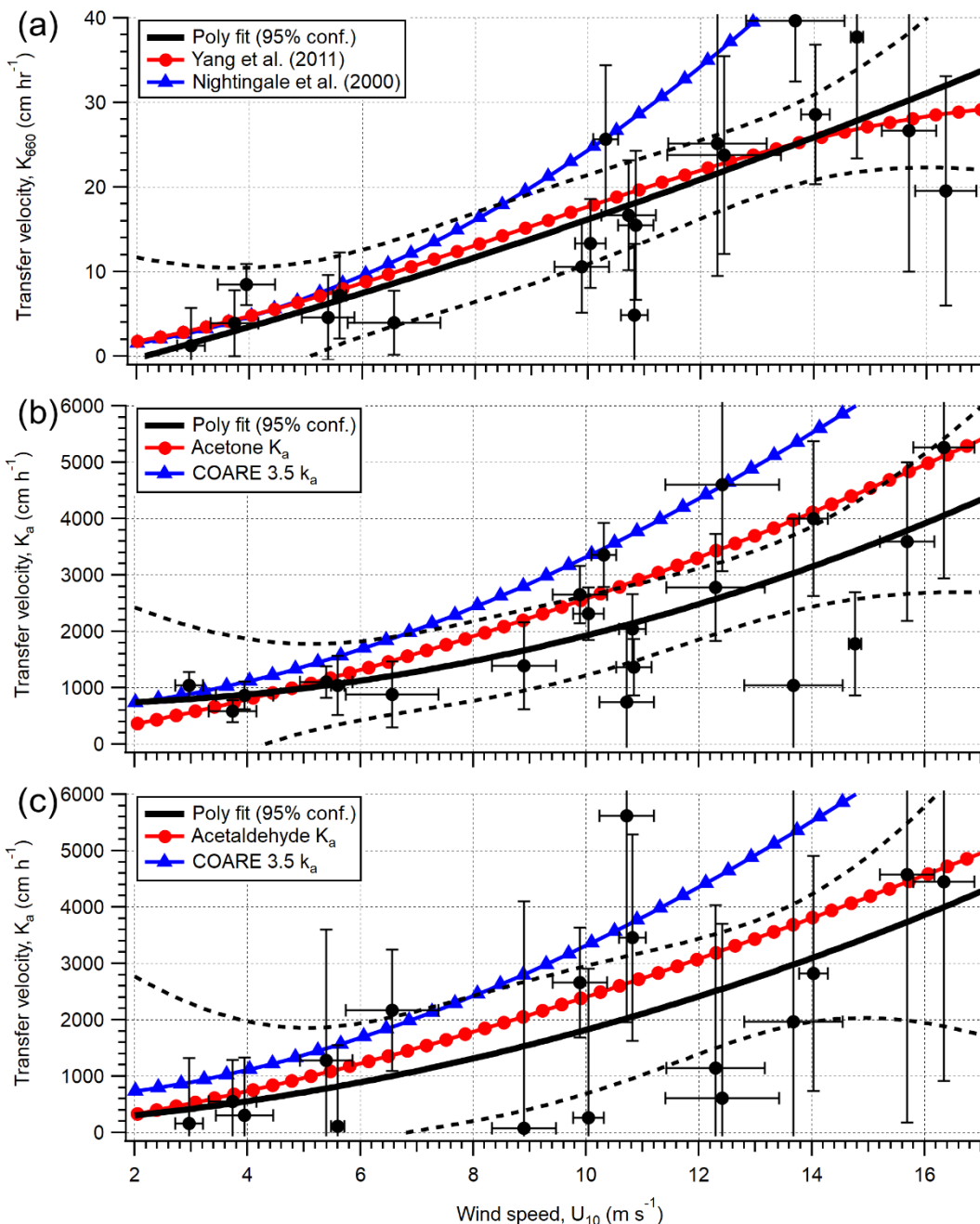


Figure 7: Calculated transfer velocities (hourly) for a) DMS ($K_{w,600}$), b) acetone (K_a), and c) acetaldehyde (K_a) in the open water footprint of the Penlee Point Atmospheric Observatory during the dates 27/04/18–03/05/18. Error bars on the experimental data (black circles) are propagated uncertainty from the eddy covariance measurement. The black poly fit lines are fit to the experimental data, with the dashed black lines representing 95 % confidence in the poly fit. The red circle and blue triangle lines in subplot A are theoretical transfer velocities using the k_w parameterisations of Yang et al. (2011a) and Nightingale et al. (2000) respectively. The red circle lines in subplots b and c are theoretical transfer velocities calculated from the k_w parameterisation of Yang et al. (2011a) and k_a from COAREG 3.5 model (shown as blue triangles).

Table 1: Eddy covariance flux measurements over the entire campaign. Errors indicate standard errors (SE) with n=135 and n=40 hour-bins for the open water and Plymouth Sound sectors respectively. Also included are the quartiles (qrt).

Compound	Open water ($\mu\text{mol m}^{-2} \text{d}^{-1}$)				Plymouth Sound ($\mu\text{mol m}^{-2} \text{d}^{-1}$)			
	25 % qrt.	Median	Mean	75 % qrt.	25 % qrt.	Median	Mean	75 % qrt.
Acetaldehyde	-7.44	-1.23	-1.55 ± 1.14	4.93	-10.86	-4.45	-4.45 ± 1.73	1.84
Acetone	-12.15	-6.27	-8.01 ± 0.77	-2.19	-17.52	-9.47	-12.93 ± 1.37	-2.19
DMS	0.79	4.05	4.67 ± 0.56	8.26	-0.96	1.16	1.75 ± 0.80	4.80
Isoprene	-3.54	0.60	1.71 ± 0.73	5.82	-8.84	-0.24	-1.95 ± 1.65	3.56

Table 2: Saturation and two-layer bulk fluxes of VOC in open water (SW) and Plymouth sound (NE) water (27/04/18–03/05/18) along with the eddy covariance measurements for this period. Errors for water concentration and air mixing ratio (measurement) and saturation (propagation) indicate one standard deviation. Errors for flux indicate one standard error.

Compound	Open water					Plymouth Sound	
	Water conc. (nM)	Air mixing ratio (ppbv)	Saturation (%)	TL flux ($\mu\text{mol m}^{-2} \text{d}^{-1}$)	EC flux ($\mu\text{mol m}^{-2} \text{d}^{-1}$)	Air mixing ratio (ppbv)	EC flux ($\mu\text{mol m}^{-2} \text{d}^{-1}$)
Acetaldehyde	7.1 \pm 1.4	0.51 \pm 0.07	44 \pm 6	-6.76 \pm 0.59	-3.94 \pm 1.23	0.75 \pm 0.04	-7.32 \pm 2.86
Acetone	5.3 \pm 2.0	0.82 \pm 0.16	15 \pm 3	-18.98 \pm 2.24	-14.93 \pm 2.09	1.09 \pm 0.09	-8.21 \pm 4.00
DMS	3.6 \pm 0.8	0.20 \pm 0.09	1434 \pm 569	9.41 \pm 1.03	9.61 \pm 1.55	0.015 \pm 0.006	2.55 \pm 2.36
Isoprene	0.09 \pm 0.01	0.18 \pm 0.05	971 \pm 221	0.30 \pm 0.05	1.65 \pm 1.89	0.28 \pm 0.03	9.27 \pm 3.01

Table A1: PTR-MS method used for measurements.

Parameter	Value
Drift chamber pressure (mBar)	2.3
Drift chamber voltage (V)	690
Drift chamber temperature (°C)	80
H_2O mass flow (mL min $^{-1}$)	5
Source/proportional valve (%)	49
Inlet flow rate (mL min $^{-1}$)	150
Inlet temperature (°C)	80

Table A2: Flux segment quality control criteria.

Parameter	Value
Wind direction, σ (°)	< 10
Momentum flux ($\text{kg m}^{-2} \text{s}^{-1}$)	< 0
Tilt angle (°)	< 15
σ_w/u_*	1.2 < x < 1.9
σ_U^2/U (m s $^{-1}$)	< 0.35

Table A3: Fresh water solubility (H^{cp}), solubility temperature dependence ($\frac{d \ln(H^{cp})}{d(1/T)}$) and molar volume (V_b) used in calculations of seawater solubility and Schmidt number at ambient temperature and salinity. H^{cp} and $d \ln(H^{cp})/d(1/T)$ for freshwater are updated from Sander (2015) and Burkholder et al. (2015).

Compound	H^{cp} (mol L $^{-1}$ atm $^{-1}$)	$\frac{d \ln(H^{cp})}{d(1/T)}$ (K)	V_b (cm 3 mol $^{-1}$)
Acetaldehyde	13.4	5775	56
Acetone	29.0	5170	77.6
DMS	0.541	3520	77
Isoprene	0.0345	4400	105

Table A4: Seawater concentrations of VOCs at the L4 marine station at 2 m depth. * denotes concentration used for two-layer calculation.

Date	Acetaldehyde (nM)	Acetone (nM)	DMS (nM)	Isoprene (nM)	Measurement method
26/03/18	8.09*	3.93*	1.11	0.09*	SFCE-PTRMS
10/04/18	-	-	2.56	-	GC
19/04/18	-	-	10.34	-	GC
23/04/18	-	-	3.03*	-	GC
30/04/18	-	-	4.13*	-	GC
21/05/18	-	-	10.69	-	GC
30/05/18	6.16*	6.71*	4.99	0.10*	SFCE-PTRMS